

## Resonances and vibrations in an elevator cable system due to boundary sway

Gaiko, Nick V.; van Horssen, Wim T.

**DOI**

[10.1016/j.jsv.2017.11.054](https://doi.org/10.1016/j.jsv.2017.11.054)

**Publication date**

2018

**Document Version**

Final published version

**Published in**

Journal of Sound and Vibration

**Citation (APA)**

Gaiko, N. V., & van Horssen, W. T. (2018). Resonances and vibrations in an elevator cable system due to boundary sway. *Journal of Sound and Vibration*, 424, 272-292. <https://doi.org/10.1016/j.jsv.2017.11.054>

**Important note**

To cite this publication, please use the final published version (if applicable).  
Please check the document version above.

**Copyright**

Other than for strictly personal use, it is not permitted to download, forward or distribute the text or part of it, without the consent of the author(s) and/or copyright holder(s), unless the work is under an open content license such as Creative Commons.

**Takedown policy**

Please contact us and provide details if you believe this document breaches copyrights.  
We will remove access to the work immediately and investigate your claim.

***Green Open Access added to TU Delft Institutional Repository***

***'You share, we take care!' - Taverne project***

**<https://www.openaccess.nl/en/you-share-we-take-care>**

Otherwise as indicated in the copyright section: the publisher is the copyright holder of this work and the author uses the Dutch legislation to make this work public.



# Resonances and vibrations in an elevator cable system due to boundary sway

Nick V. Gaiko<sup>\*</sup>, Wim T. van Horssen

Department of Mathematical Physics, Delft Institute of Applied Mathematics, Delft University of Technology, Mekelweg 4, Delft, 2628 CD, The Netherlands

## ARTICLE INFO

### Article history:

Received 20 February 2017

Revised 27 November 2017

Accepted 29 November 2017

Available online 27 March 2018

### Keywords:

Boundary sway

Time-varying length

Multiple timescales

Singular perturbation

Resonance

Averaging

## ABSTRACT

In this paper, an analytical method is presented to study an initial-boundary value problem describing the transverse displacements of a vertically moving beam under boundary excitation. The length of the beam is linearly varying in time, i.e., the axial, vertical velocity of the beam is assumed to be constant. The bending stiffness of the beam is assumed to be small. This problem may be regarded as a model describing the lateral vibrations of an elevator cable excited at its boundaries by the wind-induced building sway. Slow variation of the cable length leads to a singular perturbation problem which is expressed in slowly changing, time-dependent coefficients in the governing differential equation. By providing an interior layer analysis, infinitely many resonance manifolds are detected. Further, the initial-boundary value problem is studied in detail using a three-timescales perturbation method. The constructed formal approximations of the solutions are in agreement with the numerical results.

© 2017 Elsevier Ltd. All rights reserved.

## 1. Introduction

Within the last decade, high-rise buildings have entered a new era of “megatall” buildings, which are over 600 m in height. The construction of such tall buildings has many practical limitations due to various issues. The higher buildings rise, the more vulnerable they become to wind influence. This wind-force can lead to building sway, which can initiate the motion of elevator cables. Resonances in elevator cables can damage shaft devices or cause entanglements in the shaft. In fact, internal transportation systems play a crucial role in the building functionality. That is why considerable attention should be paid to improvement of elevator technologies to prevent any damage, and consequently downtime of elevators. However, the increasing complexity of the engineering structures increases the complexity of their analysis. Therefore, it is also important to develop advanced analytical models in order to tackle this complexity; one of which is presented in this paper.

This work is an extension of the study by Sandilo and van Horssen [1], where the lateral vibrations of an elevator cable system with a small sinusoidal excitation at its upper end was studied. The results showed that  $\mathcal{O}(\epsilon)$  excitation at the upper end of the cable resulted in  $\mathcal{O}(\sqrt{\epsilon})$  autoresonance responses. In contrast to that work, a mathematical model developed in the current paper is made closer to reality. One of the reasons is that the formulation of the problem includes bending stiffness of the cable allowing to obtain more accurate results for higher-order frequencies. The other reason is that both boundaries of the cable are excited by a harmonic function representing wind-induced sway of the building. In reality, when the building is acted upon by high velocity winds, it tends to sway in the lateral direction. This lateral motion translates into lateral motion of the cable. Note

<sup>\*</sup> Corresponding author.

E-mail address: [N.Gaiko@tudelft.nl](mailto:N.Gaiko@tudelft.nl) (N.V. Gaiko).

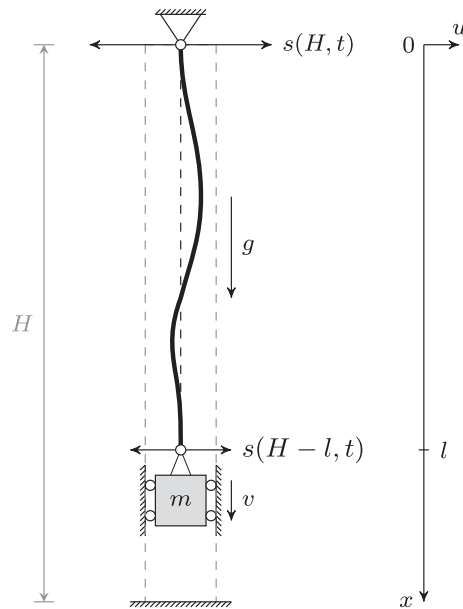


Fig. 1. Schematic of a vertically moving cable with an attached elevator car at the lower end in a swaying building.

that in our mathematical model the sway related harmonic function changes with the travel height of the elevator.

A lot of other research has been conducted on similar types of problems. Kaczmarczyk [2] analyzed resonance in a catenary-vertical cable with slowly varying length under a periodic external excitation. Zhu and Ni [3] investigated a class of axially moving continua with arbitrarily varying length. Zhu and Xu [4] studied the dynamics of elevator cables with small bending stiffness. Zhu and Teppo [5] developed a new scaled model describing the lateral vibrations of an elevator cable with a variable length for a high-rise, high-speed elevator. Kaczmarczyk and Ostachowicz derived a mathematical model [6] and provided a numerical simulation of the dynamic response [7] for transient vibrations in deep mine hoisting cables. Zhu and Chen [8] presented a control method to dissipate the vibratory energy of the cable. Moreover, the authors introduced a new experimental method to validate the theoretical results for the (un) controlled lateral vibrations. Kimura et al. [9] studied forced vibrations of an elevator rope with both ends excited by wind-induced displacement sway of the building. Kaczmarczyk [10] developed a model describing the lateral dynamics of long vertically moving ropes for high-rise transportation. Crespo et al. [11] investigated nonlinear responses of an elevator rope system coupled with the elevator car sheave motion. Bao et al. [12] studied the nonlinear response of a flexible hoisting rope with time-varying length. Gaiko and van Horssen [13] considered lateral vibrations of a vertically moving string with in time harmonically varying length.

In this paper we study, in particular, the lateral vibrations of a vertically moving beam (with linearly in time varying length) excited at both boundaries by a harmonic function in the horizontal direction (see Fig. 1). From the physical point of view, the motivation of this work is described as follows. When the fundamental frequency of the building sway matches one of the natural frequencies of elevator cable oscillations, then resonance emerges. This match happens due to a slow variation of the cable's length. In order to describe this phenomenon, an analytical methodology is developed in this paper. First, an internal layer analysis is provided to study the behavior of the solution in the neighborhood of resonance. To perform this analysis we introduce local variables in the vicinity of resonance and shift out of it on a value which follows from a certain balancing principle. Note that this value determines the size of the resonance interior layer. Next we proceed with a detailed three-timescales perturbation method. The crucial step in the construction of an approximation by this method is removing unbounded terms by providing the so-called secularity conditions. So, in order to obtain asymptotically valid approximations of the solution, one should distinguish between the behavior outside and inside resonance zones.

This paper is organized as follows. In Section 2 we make some assumptions and present an initial-boundary value problem describing the motion of the cable. Next, some transformations are introduced in order to simplify the construction of the approximation of the solution in Section 3. Further, we proceed with an internal layer analysis to study resonance in Section 4. Then, in Section 5 three-timescales are introduced to construct an accurate approximation of the solution on long timescales. Section 6 summarizes the results and provides some numerical experiments for the cable with small bending stiffness. Finally, in Section 7 we draw some conclusions based on both analytical and numerical results and also discuss future work.

## 2. Assumptions and mathematical model

In order to restrict the complexity of the analysis of the problem, it is necessary to make some assumptions:

- the mass of the cable is small compared to the mass of the elevator car (otherwise, oscillations of the building have to be coupled with the lateral motion of the elevator car);
- the elevator car is assumed to be a point mass;
- the cable is modeled as a uniform Euler-Bernoulli beam with small bending stiffness compared to its tension;
- the length of the cable is varying linearly in time, that is,  $l = l_0 + \epsilon t$ , where  $l_0$  is a constant, pretensioned length of the cable,  $\epsilon$  is a small parameter, and  $t$  is time;
- the motion of both ends of the cable in lateral direction is defined by the fundamental frequency of the building sway;
- the speed of the elevator car is smaller than the velocity of the wave propagation in the cable;
- the acceleration of the elevator car is smaller than the gravitational acceleration.

The lateral displacement,  $u$ , of the elevator cable modeled as a beam is governed by Ref. [3].

$$\rho(u_{tt} + 2vu_{xt} + v^2u_{xx} + \dot{v}u_x) - [P(x, t)u_x]_x + Elu_{xxxx} = 0, \tag{1}$$

where the overdot notation means differentiation with respect to time, and the axial loading, comprised of the car's and the cable's weights and the longitudinal acceleration, is given by

$$P(x, t) := (m + \rho[l - x])(g - \dot{v}),$$

where  $v = v(t)$  is the axial velocity of the cable,  $\rho$  is the mass-density of the cable material,  $m$  is the mass of the car,  $g$  is the gravitational acceleration,  $El$  is the flexural rigidity, where  $E$  is Young's modulus and  $I$  is the second moment of inertia of the cable section. The governing equation (1) can be rewritten as

$$\rho(u_{tt} + 2vu_{xt} + v^2u_{xx}) + \rho gu_x - P(x, t)u_{xx} + Elu_{xxxx} = 0. \tag{2}$$

In order to nondimensionalize (2), we will use the following dimensionless quantities

$$x^* = \frac{x}{L}, \quad u^* = \frac{u}{L}, \quad l^* = \frac{l}{L}, \quad \mu^* = \frac{\rho L}{m}, \quad t^* = \frac{t}{L} \sqrt{\frac{mg}{\rho}}, \quad v^* = v \sqrt{\frac{\rho}{mg}}, \quad p = \frac{1}{L^2} \frac{El}{mg}. \tag{3}$$

We also introduce the sway related term as follows (see Appendix A):

$$s(x, t) := A (\sin(\lambda x) - \sinh(\lambda x) - \alpha [\cos(\lambda x) - \cosh(\lambda x)]) \sin(\lambda^2 t), \tag{4}$$

where  $\alpha = \frac{\sin(\lambda H) + \sinh(\lambda H)}{\cos(\lambda H) + \cosh(\lambda H)}$ ,  $\lambda = \frac{1.875}{H}$  is the fundamental frequency of the building sway, and  $H$  is the elevator travel height (or a height of the building). In summary, we obtain the following initial-boundary value problem describing the vibratory dynamics of the elevator cable pinned (i.e., the rotary inertia is zero) at its boundaries. By substituting (3) into (1), omitting the asterisk notation, the dimensionless governing partial differential equation (PDE) is considered for  $0 < x < l(t)$ , and  $t > 0$  as follows:

$$u_{tt} + 2vu_{xt} + v^2u_{xx} - (\mu - \dot{v}) \left( l - x + \frac{1}{\mu} \right) u_{xx} + \mu u_x + pu_{xxxx} = 0, \tag{5a}$$

subject to the boundary conditions (BCs):

$$\begin{aligned} u(0, t) &= s(H, t), \quad \text{and} \quad u_{xx}(0, t) = 0, \\ u(l, t) &= s(H - l, t), \quad \text{and} \quad u_{xx}(l, t) = 0, \end{aligned} \tag{5b}$$

for  $t > 0$ , and with the initial conditions (ICs):

$$\begin{aligned} u(x, 0) &= f(x), \\ u_t(x, 0) &= g(x), \end{aligned} \tag{5c}$$

for  $0 < x < l_0$ . Note that according to the stated assumptions, the following orders of smallness (for the dimensionalized system parameters) will be used further in the analysis of the problem

$$\mu := \epsilon \mu_0, \quad p := \epsilon p_0, \quad A := \epsilon A_0, \quad v = \mathcal{O}(\epsilon), \quad \dot{v} = \mathcal{O}(\epsilon).$$

Note that  $\mu_0 = \frac{\mu^*}{\epsilon}$ ,  $p_0 = \frac{p}{\epsilon}$  and  $A_0$  follow from (3) and are of  $\mathcal{O}(1)$ . Initial displacement and velocity are also assumed to be small, that is

$$f = \mathcal{O}(\epsilon), \quad g = \mathcal{O}(\epsilon).$$

### 3. Problem transformation

For the sake of convenience, we slightly modify the initial-boundary value problem (5a)–(5c) in this section. First, we will introduce a space coordinate transformation in order to be able to expand the solution in a Fourier series. Then, the WKBJ method will be applied to remove the variable coefficients from the higher order terms in the initial value problem.

### 3.1. Notation

This work contains lengthy computations and sometimes some cumbersome expressions. Some of these terms are used repeatedly through out this paper. That is why we introduce the most frequent notations here. First of all, we denote the sway related terms as

$$S_0 := \frac{A_0}{l_0} \lambda^2 (\beta[1 - l_0] + \Phi(\lambda l_0)), \tag{6}$$

$$S_1(t) := \frac{A_0 \lambda^4}{l} (2\beta[1 - l] + \Phi(\lambda l)) \sin(\lambda^2 t), \tag{7}$$

$$S_2(t) := -\frac{A_0 \lambda^2}{l} (2\beta + \Phi(\lambda l)) \cos(\lambda^2 t), \tag{8}$$

where

$$\beta := \frac{\sin(\lambda H) \cosh(\lambda H) - \cos(\lambda H) \sinh(\lambda H)}{\cos(\lambda H) + \cosh(\lambda H)}, \tag{9}$$

$$\Phi(t) := -\beta[\cosh(t) + \cos(t)] - \gamma_1 \sinh(t) + \gamma_2 \sin(t), \tag{10}$$

and where

$$\gamma_i := \frac{\cos(\lambda H) \cosh(\lambda H) + (-1)^i \sin(\lambda H) \sinh(\lambda H) + 1}{\cos(\lambda H) + \cosh(\lambda H)} \quad \text{for } i = 1, 2. \tag{11}$$

Related to (7) and (8) the following functions are defined:

$$S_{k1}(t) := A_0 \lambda^4 f_k^{[1]} (2\beta[1 - l] + \Phi(\lambda l)) \sin(\lambda^2 t), \tag{12}$$

$$S_{k2}(t) := -\frac{A_0 \lambda^2 f_k^{[2]}}{l} (2\beta + \Phi(\lambda l)) \cos(\lambda^2 t), \tag{13}$$

which depend on the mode number  $k$ , and terms which will follow from orthogonality properties:

$$f_k^{[1]} := \frac{(-1)^k}{k\pi}, \quad f_k^{[2]} := \frac{1 - (-1)^k}{k\pi}, \quad f_{nk}^{[3]} := \frac{2nk}{n^2 - k^2}, \tag{14}$$

$$f_{nk}^{[4]} := [(-1)^{n+k} - 1] \frac{nk(n^2 + k^2)}{(n^2 - k^2)^2}, \quad f_{nk}^{[5]} := \frac{(-1)^{n+k} nk}{(n^2 - k^2)}, \tag{15}$$

where the superscripts are solely meant for notational purposes. In addition,

$$L_k(t) := p_0 \frac{k^2 \pi^2}{l^2} + \frac{\mu_0}{2} l. \tag{16}$$

### 3.2. A transformation to homogeneous boundary conditions on a fixed domain

The initial-boundary value problem with inhomogeneous boundary conditions can be put into a simpler form with homogeneous boundary conditions by introducing a transformation for the dependent variable. Moreover, the method of eigenfunction expansion which will be used further needs homogeneous boundary conditions. Let us use the following transformation

$$\hat{u}(x, t) := u(x, t) - s(H, t) - \frac{s(H - l, t) - s(H, t)}{l} x, \tag{17}$$

where  $s$  is given by (4). Next, we substitute (17) into (5a)–(5c), and change the spatial coordinate by  $\xi = x/l$ . Hence  $\hat{u}(x, t; \epsilon)$  becomes a new function  $\bar{u}(\xi, t; \epsilon)$ , and the initial conditions change as follows  $f(x) = \bar{f}(\xi)$  and  $g(x) = \bar{g}(\xi)$ . So, the initial-boundary value problem for  $0 < \xi < 1$  and  $t > 0$  becomes

$$\bar{u}_{tt} - \frac{1}{l^2} \bar{u}_{\xi\xi} = -\epsilon \left( \frac{p_0}{l^4} \bar{u}_{\xi\xi\xi\xi} - \frac{2}{l} (1 - \xi) \bar{u}_{\xi t} + \frac{\mu_0}{l} (1 - \xi) \bar{u}_{\xi\xi} + \frac{\mu_0}{l} \bar{u}_\xi + \xi l S_1 + S_2 \right) + \mathcal{O}(\epsilon^2), \tag{18a}$$

subject to the BCs:

$$\begin{aligned} \bar{u}(0, t; \epsilon) = \bar{u}_{\xi\xi}(0, t; \epsilon) = 0, \\ \bar{u}(1, t; \epsilon) = \bar{u}_{\xi\xi}(1, t; \epsilon) = 0, \end{aligned} \tag{18b}$$

for  $t > 0$ , and subject to the ICs:

$$\begin{aligned} \bar{u}(\xi, 0; \epsilon) &= \epsilon \bar{f}(\xi) + \mathcal{O}(\epsilon^2), \\ \bar{u}_t(\xi, 0; \epsilon) &= \epsilon \left( \bar{g}(\xi) + S_0 + \frac{\xi}{l_0} \bar{u}_\xi(\xi, 0; \epsilon) \right) + \mathcal{O}(\epsilon^2), \end{aligned} \tag{18c}$$

for  $0 < \xi < l_0$ .

### 3.3. The Fourier series expansion

In accordance with the homogeneous boundary conditions, we expand all functions in (18a)–(18c) in a Fourier sine series

$$\bar{u}(\xi, t; \epsilon) = \sum_{n=1}^{\infty} u_n(t; \epsilon) \sin(n\pi\xi). \tag{19}$$

Substituting (19) into (18a)–(18c), multiplying the so-obtained equations by  $\sin(k\pi\xi)$ , integrating with respect to  $\xi$  from 0 to 1, and using the orthogonality of the sin-functions on  $0 < \xi < 1$ , we obtain the following ordinary differential equations (ODEs) for  $k = 1, 2, 3, \dots$ , and  $t > 0$ :

$$\ddot{u}_k + \frac{k^2\pi^2}{l^2} u_k = -\epsilon \left( \frac{1}{l} \dot{u}_k + \frac{k^2\pi^2}{l^2} L_k u_k + 2S_{k1} + 2S_{k2} + \frac{2}{l} \sum_{\substack{n=1 \\ n \neq k}}^{\infty} \left[ f_{nk}^{[3]} \dot{u}_n + \mu_0 f_{nk}^{[4]} u_n \right] \right) + \mathcal{O}(\epsilon^2), \tag{20a}$$

subject to the ICs:

$$\begin{aligned} u_k(0; \epsilon) &= 2\epsilon F_k + \mathcal{O}(\epsilon^2), \\ \dot{u}_k(0; \epsilon) &= 2\epsilon \left( G_k + f_k^{[2]} S_0 + \frac{1}{l_0} \sum_{\substack{n=1 \\ n \neq k}}^{\infty} f_{nk}^{[5]} u_n(0; \epsilon) \right) + \mathcal{O}(\epsilon^2), \end{aligned} \tag{20b}$$

where  $l = l(t)$ , and the Fourier coefficients are given by

$$F_k := \int_0^1 \bar{f}(\xi) \sin(k\pi\xi) \, d\xi, \quad G_k := \int_0^1 \bar{g}(\xi) \sin(k\pi\xi) \, d\xi. \tag{21}$$

### 3.4. The Liouville-Green transformation

The homogeneous equation for (20a),

$$\ddot{u}_k + \frac{k^2\pi^2}{l^2} u_k = 0, \tag{22}$$

can be interpreted as a linear oscillator (spring) with a slowly varying restoring force. Recall that  $l = l_0 + \epsilon t$ . Equation (22) has an infinite sequence of large eigenvalues corresponding to rapid oscillations. The high oscillatory behavior implies that the variable coefficients in (22) may be approximated by constant ones over a few periods. Note that the periods are small due to large frequencies. Thus, let us approximate equation (20a) by one with constant coefficients by using the Liouville-Green transformation following from the WKBJ method [14,15]:

$$\tilde{u}(t) = \int_0^t \frac{ds}{l(s)} = \frac{1}{\epsilon} \ln \left( 1 + \frac{\epsilon t}{l_0} \right). \tag{23}$$

In accordance with a new time variable,  $u_k(t; \epsilon)$  becomes a new function  $\tilde{u}_k(\tilde{t}; \epsilon)$ . The initial-value problem (20a)–(20b) becomes

$$\frac{d^2 \tilde{u}_k}{d\tilde{t}^2} + (k\pi)^2 \tilde{u}_k = -\epsilon \left( k^2 \pi^2 \tilde{L}_k \tilde{u}_k + 2\tilde{l}^2 \left[ \tilde{S}_{k1} + \tilde{S}_{k2} \right] + 2 \sum_{\substack{n=1 \\ n \neq k}}^{\infty} \left[ f_{nk}^{[3]} \frac{d\tilde{u}_n}{d\tilde{t}} + \mu_0 f_{nk}^{[4]} \tilde{u}_n \right] \right) + \mathcal{O}(\epsilon^2), \tag{24a}$$

with the ICs:

$$\tilde{u}_k(0; \epsilon) = 2\epsilon F_k + \mathcal{O}(\epsilon^2),$$

$$\frac{d\tilde{u}_k}{dt}(0; \epsilon) = 2\epsilon \left( l_0 G_k + f_k^{[2]} l_0 S_0 + \sum_{\substack{n=1 \\ n \neq k}}^{\infty} f_{nk}^{[5]} \tilde{u}_n(0; \epsilon) \right) + \mathcal{O}(\epsilon^2), \tag{24b}$$

where  $\tilde{l} = \tilde{l}(\epsilon\tilde{t}) := l_0 e^{\epsilon\tilde{t}}$ ,  $\tilde{L}_k = \tilde{L}_k(\tilde{t}) := L_k(t)$ ,  $\tilde{S}_{k1} = \tilde{S}_{k1}(\tilde{t}) := S_{k1}(t)$ , and  $\tilde{S}_{k2} = \tilde{S}_{k2}(\tilde{t}) := S_{k2}(t)$ , where  $t(\tilde{t}) = \frac{l_0}{\epsilon} (e^{\epsilon\tilde{t}} - 1)$ .

**4. Internal layer analysis**

In this section, we determine the resonance manifolds and their corresponding timescales. Beforehand, one should observe that the terms under the summation sign in the right-hand side of (24a) are nonsecular and can be omitted. At the same time, the rest of the terms require a thorough analysis. Continuing with the analysis of the secular terms, we consider

$$\frac{d^2\tilde{u}_k}{d\tilde{t}^2} + (k\pi)^2\tilde{u}_k = -\epsilon \left( k^2\pi^2\tilde{L}_k\tilde{u}_k + 2\tilde{l}^2 [\tilde{S}_{k1} + \tilde{S}_{k2}] \right), \tag{25}$$

instead of (24a).

**4.1. Variation of constants**

When  $\epsilon = 0$ , the solution for (25) is well known, and it is given by a linear combination of  $\sin(k\pi t)$  and  $\cos(k\pi t)$ . For  $\epsilon \neq 0$ , according to the Lagrange variation of constants method [16], we assume that the general solution to equation (25) has a similar form

$$\tilde{u}_k(\tilde{t}) = A_k(\tilde{t}) \cos(k\pi\tilde{t}) + B_k(\tilde{t}) \sin(k\pi\tilde{t}), \tag{26}$$

where  $A_k$  and  $B_k$  are arbitrary functions. Further we need the following derivative

$$\frac{d\tilde{u}_k}{d\tilde{t}}(\tilde{t}) = -k\pi A_k(\tilde{t}) \sin(k\pi\tilde{t}) + k\pi B_k(\tilde{t}) \cos(k\pi\tilde{t}), \tag{27}$$

where without loss of generality were assumed that

$$\dot{A}_k \cos(k\pi\tilde{t}) + \dot{B}_k \sin(k\pi\tilde{t}) = 0. \tag{28}$$

Then, substituting (26) and (27) into (25), we obtain

$$\dot{A}_k \sin(k\pi\tilde{t}) - \dot{B}_k \cos(k\pi\tilde{t}) = \epsilon \left( k\pi\tilde{L}_k [A_k \cos(k\pi\tilde{t}) + B_k \sin(k\pi\tilde{t})] + \frac{2\tilde{l}^2}{k\pi} [\tilde{S}_{k1} + \tilde{S}_{k2}] \right). \tag{29}$$

Equations (28) and (29) constitute a system of two algebraic equations with respect to  $\dot{A}_k$  and  $\dot{B}_k$ . By solving this system and using trigonometric identities, we find

$$\begin{cases} \dot{A}_k = \epsilon \left( \frac{k\pi\tilde{L}_k}{2} [A_k \sin(2k\pi\tilde{t}) - B_k \cos(2k\pi\tilde{t})] + \frac{k\pi\tilde{L}_k}{2} B_k + \frac{2\tilde{l}^2}{k\pi} [\tilde{S}_{k1} + \tilde{S}_{k2}] \sin(k\pi\tilde{t}) \right), \\ \dot{B}_k = -\epsilon \left( \frac{k\pi\tilde{L}_k}{2} [A_k \cos(2k\pi\tilde{t}) + B_k \sin(2k\pi\tilde{t})] + \frac{k\pi\tilde{L}_k}{2} A_k + \frac{2\tilde{l}^2}{k\pi} [\tilde{S}_{k1} + \tilde{S}_{k2}] \cos(k\pi\tilde{t}) \right). \end{cases} \tag{30}$$

In (30) one should observe that the terms  $(\tilde{S}_{k1} + \tilde{S}_{k2}) \sin(k\pi\tilde{t})$  and  $(\tilde{S}_{k1} + \tilde{S}_{k2}) \cos(k\pi\tilde{t})$  contain products of trigonometric functions which lead to secular terms in  $\tilde{u}_k(\tilde{t})$ .

**4.2. Resonance manifold detection**

To study resonances in the system, we introduce the following time-like variables

$$\tau := \epsilon\tilde{t}, \quad \phi_k := k\pi\tilde{t}, \quad \psi := \frac{\lambda^2 l_0}{\epsilon} (e^\tau - 1), \quad \text{and} \quad \theta := \lambda l_0 e^\tau.$$

Note that these time-like variables monotonically increase with time. Accordingly, we rewrite system (30) as

$$\begin{cases} \dot{A}_k = \epsilon \left( \frac{k\pi\tilde{L}_k}{2} [A_k \sin 2\phi_k - B_k \cos 2\phi_k] + \frac{k\pi\tilde{L}_k}{2} B_k + \frac{2\tilde{l}^2}{k\pi} [\check{S}_{k1} \sin \psi + \check{S}_{k2} \cos \psi] \sin \phi_k \right), \\ \dot{B}_k = -\epsilon \left( \frac{k\pi\tilde{L}_k}{2} [A_k \cos 2\phi_k + B_k \sin 2\phi_k] + \frac{k\pi\tilde{L}_k}{2} A_k + \frac{2\tilde{l}^2}{k\pi} [\check{S}_{k1} \sin \psi + \check{S}_{k2} \cos \psi] \cos \phi_k \right), \end{cases} \tag{31}$$



combined with the slow/fast variables

$$\begin{cases} \dot{t} = \epsilon, & \tau(0) = 0, \\ \dot{\theta} = \epsilon \lambda l_0 e^\tau, & \theta(0) = \lambda l_0, \\ \dot{\phi}_k = k\pi, & \phi_k(0) = 0, \\ \dot{\psi} = \lambda^2 l_0 e^\tau, & \psi(0) = 0. \end{cases} \tag{32}$$

Remark that we introduced  $\theta$  more for convenience than necessity in the slow-fast analysis. Note that here the dot notation means differentiation with respect to  $\tilde{t}$  and not to  $t$ ,  $\tilde{l} = \tilde{l}(\tau)$ ,  $\tilde{L} = \tilde{L}(\tau)$ , and  $\check{S}_{k1}, \check{S}_{k2}$  are given by

$$\check{S}_{k1}(\tau, \theta) := A_0 \lambda^4 f_k^{[1]} \left( 2\beta[1 - \tilde{l}] + \Phi(\theta) \right), \tag{33}$$

$$\check{S}_{k2}(\tau, \theta) := -\frac{A_0 \lambda^2}{\tilde{l}} f_k^{[2]} (2\beta + \Phi(\theta)). \tag{34}$$

Note the last two variables  $\phi_k$  and  $\psi$  in (31) are fast-varying, while the rest,  $\tau$  and  $\theta$ , are slow. Keep in mind that the system can be averaged over the fast variables [16]. Combining  $\sin \phi_k$  and  $\cos \phi_k$  with  $\sin \psi$  and  $\cos \psi$ , we obtain the following combinations of arguments  $\phi_k + \psi, \phi_k - \psi$ . So the resonance zone is active when

$$\dot{\phi}_k - \dot{\psi} \approx 0, \tag{35}$$

corresponding to the manifold  $\tau \approx \ln \left( \frac{k\pi}{\lambda^2 l_0} \right)$ , where  $k\pi > \lambda^2 l_0$  for  $k \in \mathbb{N}$ . Note that when  $k\pi = \lambda^2 l_0$ , resonance occurs at time  $\tau = 0$  and the system can stabilize after the timescale of order  $\epsilon^{-\frac{1}{2}}$ . In case when  $k\pi < \lambda^2 l_0$ , the system is stable for that particular  $k$ -th mode. Observe that  $\phi_k, \psi$ , and  $\phi_k + \psi$  are time-like; consequently, they do not play a part in resonance. Next, the size of the emerged resonance zones has to be established. Note that this size will also be used as a new asymptotic scale in the subsequent section for the construction of a formal approximation.

### 4.3. Averaging inside the resonance zone

For the sake of convenience let us introduce the following combination argument  $\chi_k = \phi_k - \psi$ , and a distinguished parameter  $\delta(\epsilon) = o(1)$  as  $\epsilon \rightarrow 0$  to be determined later. In order to study the behavior of the solution in the resonance zone, we rescale  $\tau$  as follows:

$$\tau = \delta(\epsilon)\tau_k + \ln \left( \frac{k\pi}{\lambda^2 l_0} \right), \tag{36}$$

where  $\tau_k$  is a new local variable. Observe that

$$\dot{\chi}_k = \dot{\phi}_k - \dot{\psi}_k = -\delta(\epsilon)k\pi\tau_k + \mathcal{O}(\delta^2(\epsilon)).$$

Let us rewrite system (31), using trigonometric identities, as

$$\begin{cases} \dot{A}_k = \epsilon \left( \frac{k\pi \tilde{L}_k}{2} [A_k \sin 2\phi_k - B_k \cos 2\phi_k] + \frac{k\pi \tilde{L}_k}{2} B_k + \frac{\tilde{l}^2}{k\pi} \bar{S}_{k1} [\cos \chi_k - \cos(\phi_k + \psi_k)] + \frac{\tilde{l}^2}{k\pi} \bar{S}_{k2} [\sin \chi_k + \sin(\phi_k + \psi_k)] \right), \\ \dot{B}_k = -\epsilon \left( \frac{k\pi \tilde{L}_k}{2} [A_k \cos 2\phi_k + B_k \sin 2\phi_k] + \frac{k\pi \tilde{L}_k}{2} A_k + \frac{\tilde{l}^2}{k\pi} \bar{S}_{k1} [\sin(\phi_k + \psi_k) - \sin \chi_k] + \frac{\tilde{l}^2}{k\pi} \bar{S}_{k2} [\cos \chi_k + \cos(\phi_k + \psi_k)] \right), \end{cases}$$

combined with the slow/fast variables

$$\begin{cases} \dot{t}_k = \frac{\epsilon}{\delta(\epsilon)}, & \tau_k(0) = -\frac{1}{\delta(\epsilon)} \ln \left( \frac{k\pi}{\lambda^2 l_0} \right), \\ \dot{\theta}_k = \epsilon \lambda l_0 e^{\delta(\epsilon)\tau_k}, & \theta_k(0) = \lambda l_0, \\ \dot{\chi}_k = -\delta(\epsilon)k\pi\tau_k, & \chi_k(0) = 0, \\ \dot{\phi}_k = k\pi, & \phi_k(0) = 0, \\ \dot{\psi}_k = \lambda^2 l_0 e^{\delta(\epsilon)\tau_k}, & \psi_k(0) = 0. \end{cases} \tag{37}$$

Note the dot notation means differentiation with respect to  $\tilde{t}$ ,  $\tilde{l} = \tilde{l}(\tau_k)$ ,  $\bar{S}_{k1} = \check{S}_{k1}(\tau_k, \theta_k)$ , and  $\bar{S}_{k2} = \check{S}_{k2}(\tau_k, \theta_k)$ . In order to balance the equations of system (37), we have to choose  $\delta(\epsilon) = \sqrt{\epsilon}$ . This value determines the size of the resonance layer. With this choice, the equations for the time-like variables become

$$\dot{t}_k = \sqrt{\epsilon}, \quad \dot{\chi}_k = -\sqrt{\epsilon}k\pi\tau_k + \mathcal{O}(\epsilon), \quad \dot{\psi}_k = \lambda^2 l_0 e^{\sqrt{\epsilon}\tau_k}, \quad \text{and} \quad \dot{\theta}_k = \epsilon \lambda l_0 e^{\sqrt{\epsilon}\tau_k}. \tag{38}$$

The right-hand sides of the equations for  $A_k$  and  $B_k$  in (37) are  $2\pi$ -periodic in  $\phi_k$  and  $\psi_k$ . So let us average system (37), taking into account (38), over the fast variables. The system takes the following form

$$\begin{cases} \dot{A}_k^a = \epsilon \left( \frac{k\pi \tilde{L}_k^a}{2} B_k^a + \frac{\tilde{l}_a^2}{k\pi} [S_{k1}^a \cos \chi_k^a + S_{k2}^a \sin \chi_k^a] \right), \\ \dot{B}_k^a = -\epsilon \left( \frac{k\pi \tilde{L}_k^a}{2} A_k^a + \frac{\tilde{l}_a^2}{k\pi} [-S_{k1}^a \sin \chi_k^a + S_{k2}^a \cos \chi_k^a] \right), \end{cases} \tag{39}$$

combined with the slow/fast variables

$$\begin{cases} \dot{\tau}_k^a = \sqrt{\epsilon}, & \tau_k^a(0) = -\frac{1}{\sqrt{\epsilon}} \ln \left( \frac{k\pi}{\lambda^2 l_0} \right), \\ \dot{\theta}_k^a = \epsilon \lambda l_0 e^{\sqrt{\epsilon} \tau_k^a}, & \theta_k^a(0) = \lambda l_0, \\ \dot{\chi}_k^a = -\sqrt{\epsilon} k \pi \tau_k^a, & \chi_k^a(0) = 0, \end{cases} \tag{40}$$

where  $\tilde{l} = \tilde{l}_a(\tau_k^a)$ ,  $S_{k1}^a = \tilde{S}_{k1}^a(\tau_k^a, \theta_k^a)$ , and  $S_{k2}^a = \tilde{S}_{k2}^a(\tau_k^a, \theta_k^a)$ . Note that we have replaced  $A_k, B_k, \tau_k, \theta_k, \chi_k, \tilde{l}$ , and  $\tilde{L}_k$  by  $A_k^a, B_k^a, \tau_k^a, \theta_k^a, \chi_k^a, \tilde{l}_a$ , and  $\tilde{L}_k^a$  respectively, since the averaged equations define different vector functions but are still valid on the timescale of  $\mathcal{O}(\epsilon^{-\frac{1}{2}})$  as long as we do not leave the  $\mathcal{O}(\sqrt{\epsilon})$ -neighborhood of the resonance manifold.

#### 4.4. Averaging outside the resonance zone

Outside the resonance manifold, we average the right-hand side of the first equations in (31) over  $\phi_k$  and  $\psi$  while keeping  $A_k$  and  $B_k$  fixed. Note that second terms,  $\frac{k\pi \tilde{L}_k}{2} B_k$  and  $\frac{k\pi \tilde{L}_k}{2} A_k$ , are slowly varying, therefore they will not average out; at the same time the average of the first terms over  $\phi_k$  is zero. The last terms consist of the fast varying terms outside the resonance zone. Thus, averaging of (31) over  $\phi_k$  and  $\psi$  results in the following approximate equations

$$\begin{cases} \frac{dA_k^a}{dt} - \epsilon \frac{k\pi \tilde{L}_k^a}{2} B_k^a = 0, \\ \frac{dB_k^a}{dt} + \epsilon \frac{k\pi \tilde{L}_k^a}{2} A_k^a = 0, \end{cases} \tag{41}$$

with  $A_k^a(0) = A_k(0)$  and  $B_k^a(0) = B_k(0)$ , and where  $\tilde{L}_k^a$  is a function of  $\epsilon \tilde{t}$ . The solution of system (41) can be readily found by using the method of separation of variables, and it is given by

$$\begin{aligned} A_k^a(\tilde{t}) &= \sqrt{A_k^2(0) + B_k^2(0)} \cos \left( -\frac{k\pi}{4} r_k(\tilde{t}) + q_k \right), \\ B_k^a(\tilde{t}) &= \sqrt{A_k^2(0) + B_k^2(0)} \sin \left( -\frac{k\pi}{4} r_k(\tilde{t}) + q_k \right), \end{aligned}$$

where  $r_k$  and  $q_k$  are given by

$$\begin{aligned} r_k(\tilde{t}) &= \left( -p_0 \frac{k^2 \pi^2}{\tilde{l}^2(\epsilon \tilde{t})} + \mu_0 \tilde{l}(\epsilon \tilde{t}) \right), \\ q_k &= \arctan \left( \frac{B_k(0)}{A_k(0)} \right) + \frac{k\pi}{4} \left( -p_0 \frac{k^2 \pi^2}{\tilde{l}_0^2} + \mu_0 l_0 \right), \end{aligned}$$

for  $k \in \mathbb{N}$ .

### 5. Formal approximation

In the previous section we found that the resonances emerged repeatedly in the neighborhood of time instants  $\tau_k$  for  $k \in \mathbb{N}$ . First of all, in order to construct accurate approximations in the neighborhood of  $\tau_k$ , we rescale it as follows:

$$\tau_k = \hat{t} + \frac{1}{\epsilon} \ln \left( \frac{k\pi}{\lambda^2 l_0} \right), \tag{42}$$

where  $\hat{t}$  is a new local variable. Consequently,  $\tilde{u}_k(\tilde{t}; \epsilon)$  becomes a new function  $y_k(\hat{t}; \epsilon)$  in (24a)–(24b). Correspondingly, the initial-value problem takes the following form up to  $\mathcal{O}(\epsilon)$ . The ODE is considered for  $t > 0$ :

$$\ddot{y}_k + (k\pi)^2 y_k = -\epsilon \left( k^2 \pi^2 \hat{L}_k y_k + 2\hat{l}_k^2 [\hat{S}_{k1} + \hat{S}_{k2}] + 2 \sum_{\substack{n=1 \\ n \neq k}}^{\infty} [f_{nk}^{[3]} \dot{y}_n + \mu_0 f_{nk}^{[4]} \hat{l}_n y_n] \right), \tag{43a}$$

and subject to the ICs:

$$y_k(a_k; \epsilon) = 2\epsilon F_k, \tag{43b}$$

$$\dot{y}_k(a_k; \epsilon) = 2\epsilon \left( l_0 G_k + f_k^{[2]} l_0 S_0 + \sum_{\substack{n=1 \\ n \neq k}}^{\infty} f_{nk}^{[5]} y_n(a_n; \epsilon) \right),$$

where  $a_k := -\frac{1}{\epsilon} \ln \left( \frac{k\pi}{\lambda^2 l_0} \right)$ ,  $\hat{l}_k(\epsilon \hat{t}) := \frac{k\pi}{\lambda^2} e^{\epsilon \hat{t}}$ , and

$$\hat{L}_k(\epsilon \hat{t}) := p_0 \frac{k^2 \pi^2}{\hat{l}^2(\epsilon \hat{t})} + \frac{\mu_0 \hat{l}(\epsilon \hat{t})}{2}, \tag{44}$$

$$\hat{S}_{k1}(\hat{t}) := A_0 \lambda^4 f_k^{[1]} \left( 2\beta [1 - \hat{l}_k] + \Phi(\hat{\theta}_k) \right) \sin \hat{\psi}_k, \tag{45}$$

$$\hat{S}_{k2}(\hat{t}) := -\frac{A_0 \lambda^2 f_k^{[2]}}{\hat{l}_k} \left( 2\beta + \Phi(\hat{\theta}_k) \right) \cos \hat{\psi}_k, \tag{46}$$

where the time-like variables  $\hat{\psi}_k$  and  $\hat{\theta}_k$  have the form, respectively,

$$\hat{\psi}_k = \frac{1}{\epsilon} \left( k\pi e^{\epsilon \hat{t}} - \lambda^2 l_0 \right), \text{ and } \hat{\theta}_k = \frac{k\pi}{\lambda} e^{\epsilon \hat{t}}, \tag{47}$$

respectively.

It has been shown in the previous section that the  $\mathcal{O}(\epsilon)$  excitations produce an unexpected timescale of  $\mathcal{O} \left( \epsilon^{-\frac{1}{2}} \right)$ . Therefore we introduce the following three timescales

$$t_0 = \hat{t}, \quad t_1 = \sqrt{\epsilon \hat{t}}, \text{ and } t_2 = \epsilon \hat{t} \tag{48}$$

as natural timescales for this problem. As a consequence, the solution  $y_k(\hat{t}; \epsilon)$  is rewritten as a function of three timescales  $w_k(t_0, t_1, t_2; \sqrt{\epsilon})$ . Time derivatives of  $y_k$  will transform, correspondingly, as follows:

$$\dot{y}_k = \frac{\partial w_k}{\partial t_0} + \sqrt{\epsilon} \frac{\partial w_k}{\partial t_1} + \epsilon \frac{\partial w_k}{\partial t_2}, \tag{49}$$

$$\ddot{y}_k = \frac{\partial^2 w_k}{\partial t_0^2} + 2\sqrt{\epsilon} \frac{\partial^2 w_k}{\partial t_0 \partial t_1} + \epsilon \left( \frac{\partial^2 w_k}{\partial t_1^2} + 2 \frac{\partial^2 w_k}{\partial t_0 \partial t_2} \right) + 2\epsilon \sqrt{\epsilon} \frac{\partial^2 w_k}{\partial t_1 \partial t_2}. \tag{50}$$

As a next step, according to the three-timescales perturbation method,  $w_k(t_0, t_1, t_2; \sqrt{\epsilon})$  can be approximated by the following formal asymptotic expansion

$$w_k(t_0, t_1, t_2; \sqrt{\epsilon}) \sim \sqrt{\epsilon} w_{k0}(t_0, t_1, t_2) + \epsilon w_{k1}(t_0, t_1, t_2) + \epsilon \sqrt{\epsilon} w_{k2}(t_0, t_1, t_2) + \dots \tag{51}$$

Substituting (51) into the recently obtained initial value problem and collecting terms of like powers of  $\epsilon$ , we will obtain a set of problems of different order of smallness. Note that one has to distinguish between the solutions inside and outside the resonance zones while constructing a formal approximation.

### 5.1. The $\mathcal{O}(\sqrt{\epsilon})$ -problem

Equating the coefficients of like powers of  $\sqrt{\epsilon}$ , we obtain an equation which can be interpreted as a simple harmonic oscillator for the  $k$ -th oscillation mode of the PDE:

$$\frac{\partial^2 w_{k0}}{\partial t_0^2} + (k\pi)^2 w_{k0} = 0, \quad \text{for } t > 0, \tag{52a}$$

with the ICs:

$$\begin{aligned} w_{k0}(a_k, b_k, c_k) &= 0, \\ \frac{\partial w_{k0}}{\partial t_0}(a_k, b_k, c_k) &= 0, \end{aligned} \tag{52b}$$

where  $a_k$  is introduced in (43b),  $b_k := -\frac{\sqrt{\epsilon}}{\epsilon} \ln\left(\frac{k\pi}{\lambda^2 l_0}\right)$ , and  $c_k := -\ln\left(\frac{k\pi}{\lambda^2 l_0}\right)$ . The general solution of this problem is given by

$$w_{k0}(t_0, t_1, t_2) = A_{k0}(t_1, t_2) \cos(k\pi t_0) + B_{k0}(t_1, t_2) \sin(k\pi t_0), \tag{53}$$

where  $A_{k0}$  and  $B_{k0}$  are unknown functions yet, and can be obtained from the secularity conditions for the higher-order problems. It can be observed from the initial conditions (52b) that  $A_{k0}(b_k, c_k) = B_{k0}(b_k, c_k) = 0$ .

### 5.2. The $\mathcal{O}(\epsilon)$ -problem

By collecting terms of equal powers in  $\epsilon$ , we obtain the following problem to solve:

$$\frac{\partial^2 w_{k1}}{\partial t_0^2} + (k\pi)^2 w_{k1} = -2 \frac{\partial^2 w_{k0}}{\partial t_0 \partial t_1} - 2\hat{l}_k^2 [\hat{S}_{k1} + \hat{S}_{k2}], \quad \text{for } t > 0, \tag{54a}$$

with the ICs:

$$\begin{aligned} w_{k1}(a_k, b_k, c_k) &= 2F_k, \\ \frac{\partial w_{k1}}{\partial t_0}(a_k, b_k, c_k) &= -\frac{\partial w_{k0}}{\partial t_1}(a_k, b_k, c_k) + 2l_0 G_k - f_k^{[2]} l_0 S_0. \end{aligned} \tag{54b}$$

Using (53), we rewrite (54a) as follows:

$$\frac{\partial^2 w_{k1}}{\partial t_0^2} + (k\pi)^2 w_{k1} = 2k\pi \left[ \frac{\partial A_{k0}}{\partial t_1} \sin(k\pi t_0) - \frac{\partial B_{k0}}{\partial t_1} \cos(k\pi t_0) \right] - 2\hat{l}_k^2 [\hat{S}_{k1} + \hat{S}_{k2}]. \tag{55}$$

We will find an explicit solution for this problem inside and outside the resonance zone.

#### 5.2.1. Inside the resonance zone

First of all let us take a closer look at the functions  $\hat{S}_{k1}$  and  $\hat{S}_{k2}$  given by (45) and (46), respectively. They contain products of trigonometric functions, which might cause secular terms. These products lead to sums or differences of their arguments namely  $\hat{\psi}_k + \hat{\theta}_k$  or  $\hat{\psi}_k - \hat{\theta}_k$ , respectively. In accordance with the timescale of  $\mathcal{O}(\epsilon^{-\frac{1}{2}})$ , it is convenient to expand these arguments in a Taylor series in  $\epsilon$ :

$$\hat{\psi}_k = k\pi t_0 + \frac{1}{2} k\pi t_1^2 + \sigma_k^{[0]} + \mathcal{O}(\sqrt{\epsilon}) \text{ with } \sigma_k^{[0]} := \frac{1}{\epsilon} (k\pi - \lambda^2 l_0), \tag{56}$$

$$\hat{\psi}_k - \hat{\theta}_k = k\pi t_0 + \frac{1}{2} k\pi t_1^2 + \sigma_k^{[-]} + \mathcal{O}(\sqrt{\epsilon}) \text{ with } \sigma_k^{[-]} := \frac{1}{\epsilon} (k\pi - \lambda^2 l_0) - \frac{k\pi}{\lambda}, \tag{57}$$

$$\hat{\psi}_k + \hat{\theta}_k = k\pi t_0 + \frac{1}{2} k\pi t_1^2 + \sigma_k^{[+]} + \mathcal{O}(\sqrt{\epsilon}) \text{ with } \sigma_k^{[+]} := \frac{1}{\epsilon} (k\pi - \lambda^2 l_0) + \frac{k\pi}{\lambda}, \tag{58}$$

where  $\sigma_k^{[0]}, \sigma_k^{[-]}, \sigma_k^{[+]}$  are the phases. With these new notations, we rewrite (55) as follows

$$\frac{\partial^2 w_{k1}}{\partial t_0^2} + (k\pi)^2 w_{k1} = \left( 2k\pi \frac{\partial A_{k0}}{\partial t_1} + \hat{S}_{k1}^{[1]} - \hat{S}_{k2}^{[2]} \right) \sin(k\pi t_0) - \left( 2k\pi \frac{\partial B_{k0}}{\partial t_1} - \hat{S}_{k1}^{[2]} + \hat{S}_{k2}^{[1]} \right) \cos(k\pi t_0), \tag{59}$$

where

$$\hat{S}_{k1}^{[1]}(t_1, t_2) := A_0 \lambda^4 \hat{l}_k^2 f_k^{[1]} \left( 4\beta \hat{l}_k \cos\left(\frac{1}{2} k\pi t_1^2 + \sigma_k^{[0]}\right) - \hat{S}_{k2}^{[1]} \right), \tag{60}$$

$$\hat{S}_{k1}^{[2]}(t_1, t_2) := A_0 \lambda^4 \hat{l}_k^2 f_k^{[1]} \left( 4\beta \hat{l}_k \sin\left(\frac{1}{2} k\pi t_1^2 + \sigma_k^{[0]}\right) - \hat{S}_{k2}^{[2]} \right), \tag{61}$$

where  $\hat{l} = \hat{l}_k(t_2)$ , and

$$\begin{aligned} \hat{S}_{k2}^{[1]}(t_1, t_2) &:= 2 \left[ 2\beta - \beta \cosh \hat{\theta}_k - \gamma_1 \sinh \hat{\theta}_k \right] \cos\left(\frac{1}{2} k\pi t_1^2 + \sigma_k^{[0]}\right) + \beta \left[ \cos\left(\frac{1}{2} k\pi t_1^2 + \sigma_k^{[-]}\right) + \cos\left(\frac{1}{2} k\pi t_1^2 + \sigma_k^{[+]}\right) \right] \\ &+ \gamma_2 \left[ \sin\left(\frac{1}{2} k\pi t_1^2 + \sigma_k^{[-]}\right) - \sin\left(\frac{1}{2} k\pi t_1^2 + \sigma_k^{[+]}\right) \right], \end{aligned} \tag{62}$$

$$\widehat{S}_{k2}^{[2]}(t_1, t_2) := 2 \left[ 2\beta - \beta \cosh \widehat{\theta}_k - \gamma_1 \sinh \widehat{\theta}_k \right] \sin \left( \frac{1}{2} k\pi t_1^2 + \sigma_k^{[0]} \right) - \beta \left[ \sin \left( \frac{1}{2} k\pi t_1^2 + \sigma_k^{[-]} \right) + \sin \left( \frac{1}{2} k\pi t_1^2 + \sigma_k^{[+]} \right) \right] + \gamma_2 \left[ \cos \left( \frac{1}{2} k\pi t_1^2 + \sigma_k^{[-]} \right) - \cos \left( \frac{1}{2} k\pi t_1^2 + \sigma_k^{[+]} \right) \right]. \tag{63}$$

The solution  $w_{k1}$  produces unbounded terms in  $t_0$  unless

$$\frac{\partial A_{k0}}{\partial t_1} + \frac{1}{2k\pi} \left( \widehat{S}_{k1}^{[1]} - \widehat{S}_{k2}^{[2]} \right) = 0, \tag{64}$$

$$\frac{\partial B_{k0}}{\partial t_1} - \frac{1}{2k\pi} \left( \widehat{S}_{k1}^{[2]} + \widehat{S}_{k2}^{[1]} \right) = 0. \tag{65}$$

By straightforward integration we obtain

$$A_{k0}(t_1, t_2) = -\frac{A_0 \lambda^4 \widehat{I}_k}{2k\sqrt{k\pi}} \left( f_k^{[1]} \widehat{I}_{k1}^{[1]} + f_k^{[2]} \widehat{I}_{k2}^{[2]} \right) + C_{k0}(t_2), \tag{66}$$

$$B_{k0}(t_1, t_2) = \frac{A_0 \lambda^4 \widehat{I}_k}{2k\sqrt{k\pi}} \left( f_k^{[1]} \widehat{I}_{k1}^{[2]} + f_k^{[2]} \widehat{I}_{k2}^{[1]} \right) + D_{k0}(t_2), \tag{67}$$

where  $C_{k0}$  and  $D_{k0}$  are unknown functions which can be obtained from the  $\mathcal{O}(\epsilon\sqrt{\epsilon})$ -problem, and where

$$\widehat{I}_{k1}^{[1]}(t_1, t_2) := \widehat{I}_k \left[ 4\beta \widehat{I}_k \left( \cos \sigma_k^{[0]} C_{Fr}(\sqrt{kt_1}) - \sin \sigma_k^{[0]} S_{Fr}(\sqrt{kt_1}) \right) - \widehat{I}_{k2}^{[1]} \right], \tag{68}$$

$$\widehat{I}_{k1}^{[2]}(t_1, t_2) := \widehat{I}_k \left[ 4\beta \widehat{I}_k \left( \cos \sigma_k^{[0]} S_{Fr}(\sqrt{kt_1}) + \sin \sigma_k^{[0]} C_{Fr}(\sqrt{kt_1}) \right) + \widehat{I}_{k2}^{[2]} \right], \tag{69}$$

where

$$\widehat{I}_{k2}^{[1]}(t_1, t_2) := 2 \left[ 2\beta - \beta \cosh \widehat{\theta}_k - \gamma_1 \sinh \widehat{\theta}_k \right] \left[ \cos \sigma_k^{[0]} C_{Fr}(\sqrt{kt_1}) - \sin \sigma_k^{[0]} S_{Fr}(\sqrt{kt_1}) \right] - \beta \left[ (\cos \sigma_k^{[-]} + \cos \sigma_k^{[+]}) C_{Fr}(\sqrt{kt_1}) - (\sin \sigma_k^{[-]} + \sin \sigma_k^{[+]}) S_{Fr}(\sqrt{kt_1}) \right] - \gamma_2 \left[ (\cos \sigma_k^{[-]} - \cos \sigma_k^{[+]}) S_{Fr}(\sqrt{kt_1}) + (\sin \sigma_k^{[-]} - \sin \sigma_k^{[+]}) C_{Fr}(\sqrt{kt_1}) \right], \tag{70}$$

$$\widehat{I}_{k2}^{[2]}(t_1, t_2) := -2 \left[ 2\beta - \beta \cosh \widehat{\theta}_k - \gamma_1 \sinh \widehat{\theta}_k \right] \left[ \cos \sigma_k^{[0]} S_{Fr}(\sqrt{kt_1}) + \sin \sigma_k^{[0]} C_{Fr}(\sqrt{kt_1}) \right] + \beta \left[ (\cos \sigma_k^{[-]} + \cos \sigma_k^{[+]}) S_{Fr}(\sqrt{kt_1}) + (\sin \sigma_k^{[-]} + \sin \sigma_k^{[+]}) C_{Fr}(\sqrt{kt_1}) \right] - \gamma_2 \left[ (\cos \sigma_k^{[-]} - \cos \sigma_k^{[+]}) C_{Fr}(\sqrt{kt_1}) - (\sin \sigma_k^{[-]} - \sin \sigma_k^{[+]}) S_{Fr}(\sqrt{kt_1}) \right], \tag{71}$$

where  $S_{Fr}$  and  $C_{Fr}$  are the Fresnel integrals given by

$$S_{Fr}(t) := \int_0^t \sin \left( \frac{1}{2} \pi x^2 \right) dx, \text{ and } C_{Fr}(t) := \int_0^t \cos \left( \frac{1}{2} \pi x^2 \right) dx. \tag{72}$$

Actually the presence of the Fresnel integrals in the expressions for amplitudes of vibrations cause resonance jumps in the system causing the effect of autoresonance. These integrals are plotted for the third oscillation mode with  $l_0 = 0.7$  and  $\lambda = 1.875$  in Fig. 2.

### 5.2.2. Outside the resonance zone

It should be observed that the last two terms in (55) do not give rise to secular terms in  $w_{k1}$ . To prevent secular terms there,  $A_{k0}$  and  $B_{k0}$  have to satisfy the following conditions

$$\frac{\partial A_{k0}}{\partial t_1} = 0, \text{ and } \frac{\partial B_{k0}}{\partial t_1} = 0, \tag{73}$$

which have, respectively, the following solutions

$$A_{k0}(t_1, t_2) = \widetilde{C}_{k0}(t_2), \text{ and } B_{k0}(t_1, t_2) = \widetilde{D}_{k0}(t_2), \tag{74}$$

where  $\widetilde{C}_{k0}$  and  $\widetilde{D}_{k0}$  are unknown functions and can be obtained by removing secular terms from the  $\mathcal{O}(\epsilon\sqrt{\epsilon})$ -problem. From the initial conditions (52b), it follows that  $\widetilde{C}_{k0}(c_k) = \widetilde{D}_{k0}(c_k) = 0$ .

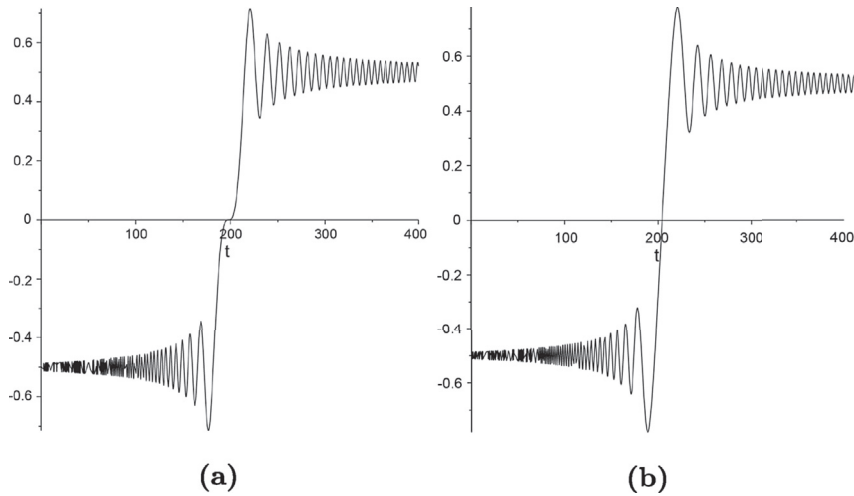


Fig. 2. Fresnel integrals (a)  $S_{Fr}$  and (b)  $C_{Fr}$  for the third oscillation mode ( $k = 3$ ).

5.2.3. General solution

Taking into account the secularity conditions (64) and (65), the general solution for (54a) is given by

$$w_{k1}(t_0, t_1, t_2) = A_{k1}(t_1, t_2) \cos(k\pi t_0) + B_{k1}(t_1, t_2) \sin(k\pi t_0), \tag{75}$$

where  $A_{k1}$  and  $B_{k1}$  are unknown functions and may be determined from higher-order problems. The initial values of  $A_{k1}$  and  $B_{k1}$  are found from the initial conditions (54b) as follows:

$$A_{k1}(b_k, c_k) = 2F_k \cos(k\pi a_k) + \frac{\sin(k\pi a_k)}{k\pi} \left( \frac{\partial A_{k0}}{\partial t_1}(b_k, c_k) \cos(k\pi a_k) + \frac{\partial B_{k0}}{\partial t_1}(b_k, c_k) \sin(k\pi a_k) - 2l_0 G + f_k^{[2]} l_0 S_0 \right), \tag{76}$$

$$B_{k1}(b_k, c_k) = 2F_k \sin(k\pi a_k) - \frac{\cos(k\pi a_k)}{k\pi} \left( \frac{\partial A_{k0}}{\partial t_1}(b_k, c_k) \cos(k\pi a_k) + \frac{\partial B_{k0}}{\partial t_1}(b_k, c_k) \sin(k\pi a_k) - 2l_0 G + f_k^{[2]} l_0 S_0 \right), \tag{77}$$

where, inside the resonance manifold,

$$\frac{\partial A_{k0}}{\partial t_1}(b_k, c_k) = -\frac{1}{2k\pi} \left( \widehat{S}_{k1}^{[1]}(b_k, c_k) - \widehat{S}_{k2}^{[2]}(b_k, c_k) \right), \tag{78}$$

$$\frac{\partial B_{k0}}{\partial t_1}(b_k, c_k) = \frac{1}{2k\pi} \left( \widehat{S}_{k1}^{[2]}(b_k, c_k) + \widehat{S}_{k2}^{[1]}(b_k, c_k) \right), \tag{79}$$

where  $\widehat{S}_{k1}^{[i]}$  and  $\widehat{S}_{k2}^{[i]}$  for  $i = 1, 2$  are given by (60)–(63). Outside the resonance manifold,  $\frac{\partial A_{k0}}{\partial t_1}(b_k, c_k)$  and  $\frac{\partial B_{k0}}{\partial t_1}(b_k, c_k)$  are equal to zero.

5.3. The  $\mathcal{O}(\epsilon\sqrt{\epsilon})$ -problem

Here we collect terms of equal powers of  $\epsilon^{\frac{3}{2}}$  and consider the last problem in this paper finalizing the construction of the formal approximation:

$$\frac{\partial^2 w_{k2}}{\partial t_0^2} + (k\pi)^2 w_{k2} = -2 \frac{\partial^2 w_{k1}}{\partial t_0 \partial t_1} - 2 \frac{\partial^2 w_{k0}}{\partial t_0 \partial t_2} - \frac{\partial^2 w_{k0}}{\partial t_1^2} - (k\pi)^2 \widehat{L}_k w_{k0} + 2 \sum_{\substack{n=1 \\ n \neq k}}^{\infty} \left( f_{nk}^{[3]} \frac{\partial w_{n0}}{\partial t_0} + \mu_0 f_{nk}^{[4]} \widehat{L}_n w_{n0} \right), \quad \text{for } t > 0, \tag{80a}$$

subject to the ICs:

$$w_{k2}(a_k, b_k, c_k) = 0, \tag{80b}$$

$$\frac{\partial w_{k2}}{\partial t_0}(a_k, b_k, c_k) = -\frac{\partial w_{k1}}{\partial t_1}(a_k, b_k, c_k) - \frac{\partial w_{k0}}{\partial t_2}(a_k, b_k, c_k).$$

Substituting (53) and (75) into (80a) and rearranging the so-obtained equation, we obtain

$$\begin{aligned} \frac{\partial^2 w_{k2}}{\partial t_0^2} + (k\pi)^2 w_{k2} &= 2k\pi \left( \frac{\partial A_{k1}}{\partial t_1} + \frac{\partial A_{k0}}{\partial t_2} - \frac{1}{2k\pi} \frac{\partial B_{k0}^2}{\partial t_1^2} - \frac{k\pi}{2} \widehat{L}_k B_{k0} \right) \sin(k\pi t_0) \\ &\quad - 2k\pi \left( \frac{\partial B_{k1}}{\partial t_1} + \frac{\partial B_{k0}}{\partial t_2} + \frac{1}{2k\pi} \frac{\partial A_{k0}^2}{\partial t_1^2} + \frac{k\pi}{2} \widehat{L}_k A_{k0} \right) \cos(k\pi t_0) \\ &\quad + 2 \sum_{\substack{n=1 \\ n \neq k}}^{\infty} \left( (\mu_0 f_{nk}^{[4]}\widehat{I}_n B_{n0} - n\pi f_{nk}^{[3]}A_{n0}) \sin(n\pi t_0) + (\mu_0 f_{nk}^{[4]}\widehat{I}_n A_{n0} + n\pi f_{nk}^{[3]}B_{n0}) \cos(n\pi t_0) \right). \end{aligned} \tag{81}$$

Next, we analyze this equation inside and outside the resonance manifold.

5.3.1. Inside the resonance zone

$$\begin{aligned} \frac{\partial^2 w_{k2}}{\partial t_0^2} + (k\pi)^2 w_{k2} &= 2k\pi \left( \frac{\partial A_{k1}}{\partial t_1} + \frac{\partial A_{k0}}{\partial t_2} - \frac{1}{2k\pi} \frac{\partial B_{k0}^2}{\partial t_1^2} - \frac{k\pi}{2} \widehat{L}_k B_{k0} \right) \sin(k\pi t_0) \\ &\quad - 2k\pi \left( \frac{\partial B_{k1}}{\partial t_1} + \frac{\partial B_{k0}}{\partial t_2} + \frac{1}{2k\pi} \frac{\partial A_{k0}^2}{\partial t_1^2} + \frac{k\pi}{2} \widehat{L}_k A_{k0} \right) \cos(k\pi t_0) + \text{“NST”}, \end{aligned} \tag{82}$$

where “NST” stands for nonsecular terms. Substituting (66) and (67) into (82), we obtain the following secularity conditions:

$$\begin{aligned} \frac{dC_{k0}}{dt_2} - \frac{k\pi}{2} \widehat{L}_k D_{k0} + \frac{\partial A_{k1}}{\partial t_1} + \frac{A_0 \lambda^2 \widehat{I}_k}{\sqrt{k}} \left\{ \frac{1}{2k\pi} \left( \lambda^2 \widehat{I}_{kf}^{[11]} \frac{\partial \widehat{I}_{k2}^{[11]}}{\partial t_2} - f_k^{[2]} \frac{\partial \widehat{I}_{k2}^{[2]}}{\partial t_2} \right) - \frac{\widehat{L}_k f_k^{[2]}}{4} (\widehat{I}_{k2}^{[2]} + \widehat{I}_{k2}^{[1]}) \right. \\ \left. - \frac{1}{4(k\pi)^2} \left( \lambda^2 \widehat{I}_{kf}^{[11]} \left[ 4k\sqrt{k\pi} \beta \widehat{I}_{kt_1} \cos\left(\frac{1}{2}k\pi t_1^2 + \sigma^{[0]}\right) + \frac{\partial^2 \widehat{I}_{k2}^{[2]}}{\partial t_1^2} \right] - f_k^{[2]} \frac{\partial^2 \widehat{I}_{k2}^{[1]}}{\partial t_1^2} \right) \right\} = 0, \end{aligned} \tag{83}$$

and

$$\begin{aligned} \frac{dD_{k0}}{dt_2} + \frac{k\pi}{2} \widehat{L}_k C_{k0} + \frac{\partial B_{k1}}{\partial t_1} + \frac{A_0 \lambda^2 \widehat{I}_k}{\sqrt{k}} \left\{ \frac{1}{2k\pi} \left( \lambda^2 \widehat{I}_{kf}^{[11]} \frac{\partial \widehat{I}_{k2}^{[2]}}{\partial t_2} + f_k^{[2]} \frac{\partial \widehat{I}_{k2}^{[1]}}{\partial t_2} \right) + \frac{\widehat{L}_k f_k^{[2]}}{4} (\widehat{I}_{k2}^{[1]} + \widehat{I}_{k2}^{[2]}) \right. \\ \left. - \frac{1}{4(k\pi)^2} \left( \lambda^2 \widehat{I}_{kf}^{[11]} \left[ 4k\sqrt{k\pi} \beta \widehat{I}_{kt_1} \sin\left(\frac{1}{2}k\pi t_1^2 + \sigma^{[0]}\right) + \frac{\partial^2 \widehat{I}_{k2}^{[1]}}{\partial t_1^2} \right] - f_k^{[2]} \frac{\partial^2 \widehat{I}_{k2}^{[2]}}{\partial t_1^2} \right) \right\} = 0. \end{aligned} \tag{84}$$

Observe that integration of these equations with respect to  $t_1$  produces unbounded solutions because of  $t_2$  depending terms. Hence, from (83) and (84) the secularity conditions follow:

$$\begin{cases} \frac{dC_{k0}}{dt_2} - \frac{k\pi}{2} \widehat{L}_k D_{k0} = 0, \\ \frac{dD_{k0}}{dt_2} + \frac{k\pi}{2} \widehat{L}_k C_{k0} = 0, \end{cases} \tag{85}$$

together with

$$\begin{aligned} \frac{\partial A_{k1}}{\partial t_1} + \frac{A_0 \lambda^2 \widehat{I}_k}{\sqrt{k}} \left\{ \frac{1}{2k\pi} \left( \lambda^2 \widehat{I}_{kf}^{[11]} \frac{\partial \widehat{I}_{k2}^{[11]}}{\partial t_2} - f_k^{[2]} \frac{\partial \widehat{I}_{k2}^{[2]}}{\partial t_2} \right) - \frac{\widehat{L}_k f_k^{[2]}}{4} (\widehat{I}_{k2}^{[2]} + \widehat{I}_{k2}^{[1]}) \right. \\ \left. - \frac{1}{4(k\pi)^2} \left( \lambda^2 \widehat{I}_{kf}^{[11]} \left[ 4k\sqrt{k\pi} \beta \widehat{I}_{kt_1} \cos\left(\frac{1}{2}k\pi t_1^2 + \sigma_k^{[0]}\right) + \frac{\partial^2 \widehat{I}_{k2}^{[2]}}{\partial t_1^2} \right] - f_k^{[2]} \frac{\partial^2 \widehat{I}_{k2}^{[1]}}{\partial t_1^2} \right) \right\} = 0, \end{aligned} \tag{86}$$

and

$$\begin{aligned} \frac{\partial B_{k1}}{\partial t_1} + \frac{A_0 \lambda^2 \widehat{I}_k}{\sqrt{k}} \left\{ \frac{1}{2k\pi} \left( \lambda^2 \widehat{I}_{kf}^{[11]} \frac{\partial \widehat{I}_{k2}^{[2]}}{\partial t_2} + f_k^{[2]} \frac{\partial \widehat{I}_{k2}^{[1]}}{\partial t_2} \right) + \frac{\widehat{L}_k f_k^{[2]}}{4} (\widehat{I}_{k2}^{[1]} + \widehat{I}_{k2}^{[2]}) \right. \\ \left. - \frac{1}{4(k\pi)^2} \left( \lambda^2 \widehat{I}_{kf}^{[11]} \left[ 4k\sqrt{k\pi} \beta \widehat{I}_{kt_1} \sin\left(\frac{1}{2}k\pi t_1^2 + \sigma_k^{[0]}\right) + \frac{\partial^2 \widehat{I}_{k2}^{[1]}}{\partial t_1^2} \right] - f_k^{[2]} \frac{\partial^2 \widehat{I}_{k2}^{[2]}}{\partial t_1^2} \right) \right\} = 0, \end{aligned} \tag{87}$$

where  $\hat{L}_k = \hat{L}_k(t_2)$  is given by (44).  $A_{k1}$  and  $B_{k1}$  can be readily found by straightforward integration of (86) and (87), but we omit the details because of cumbersome expressions. One should only observe that after integration, the arbitrary functions depending on  $t_2$  appear in the expressions for  $A_{k1}$  and  $B_{k1}$ . These functions may be determined from the  $\mathcal{O}(\epsilon^2)$ -problem. Similar to (41), system (85) can be readily solved analytically. Imposing the secularity conditions, we obtain the following inhomogeneous equation inside the resonance zone

$$\frac{\partial^2 w_{k2}}{\partial t_0^2} + (k\pi)^2 w_{k2} = 2 \sum_{\substack{n=1 \\ n \neq k}}^{\infty} \left( \left( \mu_0 f_{nk}^{[4]} \hat{L}_n B_{n0} - n\pi f_{nk}^{[3]} A_{n0} \right) \sin(n\pi t_0) + \left( \mu_0 f_{nk}^{[4]} \hat{L}_n A_{n0} + n\pi f_{nk}^{[3]} B_{n0} \right) \cos(n\pi t_0) \right). \tag{88}$$

The solution of this equation readily follows

$$w_{k2} = A_{k2} \cos(k\pi t_0) + B_{k2} \sin(k\pi t_0) + 2 \sum_{\substack{n=1 \\ n \neq k}}^{\infty} \frac{1}{\pi^2(k^2 - n^2)} \left( \left( \mu_0 f_{nk}^{[4]} \hat{L}_n B_{n0} - n\pi f_{nk}^{[3]} A_{n0} \right) \sin(n\pi t_0) + \left( \mu_0 f_{nk}^{[4]} \hat{L}_n A_{n0} + n\pi f_{nk}^{[3]} B_{n0} \right) \cos(n\pi t_0) \right), \tag{89}$$

where  $A_{k2}$  and  $B_{k2}$  are arbitrary functions of  $(t_1, t_2)$  which can be determined from the solution  $w_{k3}(t_0, t_1, t_2)$ , and where  $A_{n0}$  and  $B_{n0}$  are given by (66) and (67), respectively.

5.3.2. Outside the resonance zone

In the  $\mathcal{O}(\epsilon)$ -problem we obtained that outside the resonance zone  $A_{k0} = \tilde{C}_{k0}(t_2)$ , and  $B_{k0} = \tilde{D}_{k0}(t_2)$ ; see (74). Hence, (81) takes the following form

$$\frac{\partial^2 w_{k2}}{\partial t_0^2} + (k\pi)^2 w_{k2} = 2k\pi \left( \frac{\partial A_{k1}}{\partial t_1} + \frac{d\tilde{C}_{k0}}{dt_2} - \frac{k\pi}{2} \hat{L}_k \tilde{D}_{k0} \right) \sin(k\pi t_0) - 2k\pi \left( \frac{\partial B_{k1}}{\partial t_1} + \frac{d\tilde{D}_{k0}}{dt_2} + \frac{k\pi}{2} \hat{L}_k \tilde{C}_{k0} \right) \cos(k\pi t_0) + \text{“NST”}. \tag{90}$$

To avoid secular terms the following should hold

$$\frac{\partial A_{k1}}{\partial t_1} + \frac{d\tilde{C}_{k0}}{dt_2} - \frac{k\pi}{2} \hat{L}_k \tilde{D}_{k0} = 0, \tag{91}$$

$$\frac{\partial B_{k1}}{\partial t_1} + \frac{d\tilde{D}_{k0}}{dt_2} + \frac{k\pi}{2} \hat{L}_k \tilde{C}_{k0} = 0. \tag{92}$$

Likewise in the previous case, solving these equations with respect to  $t_1$  will produce unbounded solutions because of  $t_2$  depending terms unless  $\tilde{C}_{k0}$  and  $\tilde{D}_{k0}$  satisfy to

$$\begin{cases} \frac{d\tilde{C}_{k0}}{dt_2} - \frac{k\pi}{2} \hat{L}_k \tilde{D}_{k0} = 0, \\ \frac{d\tilde{D}_{k0}}{dt_2} + \frac{k\pi}{2} \hat{L}_k \tilde{C}_{k0} = 0, \end{cases} \tag{93}$$

where  $\hat{L}_k = \hat{L}_k(t_2)$  is given by (44). Similar to (41), this system can be solved analytically. Then, from (91) and (92) it follows that

$$\frac{\partial A_{k1}}{\partial t_1} = 0, \quad \text{and} \quad \frac{\partial B_{k1}}{\partial t_1} = 0, \tag{94}$$

for which the solutions are given by  $A_{k1}(t_1, t_2) = \tilde{C}_{k1}(t_2)$ , and  $B_{k1}(t_1, t_2) = \tilde{D}_{k1}(t_2)$ , respectively, where  $\tilde{C}_{k1}$  and  $\tilde{D}_{k1}$  are arbitrary functions which can be determined from the  $\mathcal{O}(\epsilon^2)$ -problem. Employing the secularity conditions (89), we obtain the following inhomogeneous equation outside the resonance zone

$$\frac{\partial^2 w_{k2}}{\partial t_0^2} + (k\pi)^2 w_{k2} = 2 \sum_{\substack{n=1 \\ n \neq k}}^{\infty} \left( \left( \mu_0 f_{nk}^{[4]} \hat{L}_n \tilde{D}_{n0} - n\pi f_{nk}^{[3]} \tilde{C}_{n0} \right) \sin(n\pi t_0) + \left( \mu_0 f_{nk}^{[4]} \hat{L}_n \tilde{C}_{n0} + n\pi f_{nk}^{[3]} \tilde{D}_{n0} \right) \cos(n\pi t_0) \right). \tag{95}$$

The solution has a similar form as the solution inside the resonance zone:

$$w_{k2} = \tilde{A}_{k2} \cos(k\pi t_0) + \tilde{B}_{k2} \sin(k\pi t_0) + 2 \sum_{\substack{n=1 \\ n \neq k}}^{\infty} \frac{1}{\pi^2(k^2 - n^2)} \left( \left( \mu_0 f_{nk}^{[4]} \hat{L}_n \tilde{D}_{n0} - n\pi f_{nk}^{[3]} \tilde{C}_{n0} \right) \sin(n\pi t_0) \right.$$



$$+ \left( \mu_0 f_{nk}^{[4]} \widehat{I}_n \widetilde{C}_{n0} + n\pi f_{nk}^{[3]} \widetilde{D}_{n0} \right) \cos(n\pi t_0), \tag{96}$$

where  $\widetilde{A}_{k2}$  and  $\widetilde{B}_{k2}$  are arbitrary functions of  $(t_1, t_2)$  which can be determined from the solution  $w_{k3}(t_0, t_1, t_2)$ .

**6. Results**

In this section, we summarize the results obtained in the previous section. Besides, we compute the lateral displacements and the vibratory energy of the cable by using the constructed formal approximation as well as by applying a numerical scheme to present some numerical results.

**6.1. Analytic approximation**

**6.1.1. Analytic results**

All in all, we constructed a formal approximation in the form (51) for  $\widetilde{u}_k(\widetilde{t}; \sqrt{\epsilon})$ . Introducing the following notation

$$\omega_n(t) := \frac{1}{\epsilon} \ln \left( \frac{\lambda^2(l_0 + \epsilon t)}{n\pi} \right), \tag{97}$$

and using (23) and (42), we finally obtain the approximate solution of the initial-boundary value problem (18a)–(18c) as

$$\bar{u}(x, t, t_1, t_2; \epsilon) = \sum_{n=1}^{\infty} \left( \sqrt{\epsilon} u_{n0}(t, t_1, t_2) + \epsilon u_{n1}(t, t_1, t_2) + \epsilon \sqrt{\epsilon} u_{n2}(t, t_1, t_2) \right) \times \sin \left( \frac{n\pi x}{l_0 + \epsilon t} \right), \tag{98}$$

where  $t_1$  and  $t_2$  are given by (48), and where

$$u_{n0}(t, t_1, t_2) = A_{n0}(t_1, t_2) \cos(n\pi\omega_n(t)) + B_{n0}(t_1, t_2) \sin(n\pi\omega_n(t)), \tag{99}$$

where functions  $A_{n0}$  and  $B_{n0}$  are given by (66) and (67);

$$u_{n1}(t, t_1, t_2) = A_{n1}(t_1, t_2) \cos(n\pi\omega_n(t)) + B_{n1}(t_1, t_2) \sin(n\pi\omega_n(t)), \tag{100}$$

where functions  $A_{n1}$  and  $B_{n1}$  are given by (86) and (87);

$$u_{n2}(t, t_1, t_2) = A_{n2}(t_1, t_2) \cos(n\pi\omega_n(t)) + B_{n2}(t_1, t_2) \sin(n\pi\omega_n(t)) + 2 \sum_{\substack{k=1 \\ k \neq n}}^{\infty} \frac{1}{\pi^2(n^2 - k^2)} \left[ \left( \mu_0 f_{kn}^{[4]} \widehat{I} B_{k0}(t_1, t_2) - k\pi f_{kn}^{[3]} A_{k0}(t_1, t_2) \right) \times \sin \omega_k(t) + \left( \mu_0 f_{kn}^{[4]} \widehat{I} A_{k0}(t_1, t_2) + k\pi f_{kn}^{[3]} B_{k0}(t_1, t_2) \right) \cos \omega_k(t) \right], \tag{101}$$

where functions  $A_{n2}$  and  $B_{n2}$  can be found from higher-order approximations.

Remark that the constructed formal approximations are asymptotic. Their accuracy is strongly connected with the timescales. Thus,  $u_n - (\sqrt{\epsilon} u_{n0} + \epsilon u_{n1} + \epsilon \sqrt{\epsilon} u_{n2}) = \mathcal{O}(\epsilon^2)$ ,  $u_n - (\sqrt{\epsilon} u_{n0} + \epsilon u_{n1}) = \mathcal{O}(\epsilon \sqrt{\epsilon})$ , and  $u_n - \sqrt{\epsilon} u_{n0} = \mathcal{O}(\epsilon)$  on a timescale of order  $\epsilon^{-1}$  for  $n \in \mathbb{N}$ , where  $u_n$  is given by (19). It is worth mentioning that (98) is a convergent series. An interested reader can observe that, for example,  $\mathcal{O}(\sqrt{\epsilon})$  term in (98) is similar to  $\sum_{n=1}^{\infty} \frac{\sqrt{\epsilon}}{n^{5/2}} \sin \left( \frac{n\pi x}{l_0 + \epsilon t} \right)$  which is convergent.

**6.1.2. Numerical results**

The numerical results simulating the vibration response and the energy are computed based on the analytical expressions (98), (99), and (117), respectively. The computations are performed by using the following parameters  $\epsilon = 0.01$ ,  $H = 1$ ,  $\lambda = 1.875$ ,  $l_0 = 0.7$ ,  $A_0 = 1$ . For simplicity, let us assume only the initial displacement is prescribed, so that  $f = \epsilon \sin^2 \pi \xi$ , and the initial velocity  $g = 0$  for  $0 \leq \xi \leq 1$ . In numerical computations we neglect bending stiffness of the cable because its contribution is assumed to be small. It is also worth mentioning that the following numerical results are computed based on  $\mathcal{O}(\epsilon)$  approximations. Higher-order approximations are neglected due to their insignificant contribution into the solution. By using (23) and (42), we obtain that the resonance occurs periodically in time at time instants

$$T_k = \frac{1}{\epsilon} \left( \frac{k\pi}{\lambda^2} - l_0 \right) \text{ for } k \in \mathbb{N}, \tag{102}$$

with an interval

$$\Delta T = \frac{\pi}{\epsilon \lambda^2}. \tag{103}$$

Note that the resonance time depends on the mode number  $k$ . For the first three oscillation modes, resonance emerges at times  $T_1 \approx 19.36$ ,  $T_2 \approx 108.72$ , and  $T_3 \approx 198.08$  with  $\Delta T = 89.36$ . They are illustrated in Figs. 3–6.

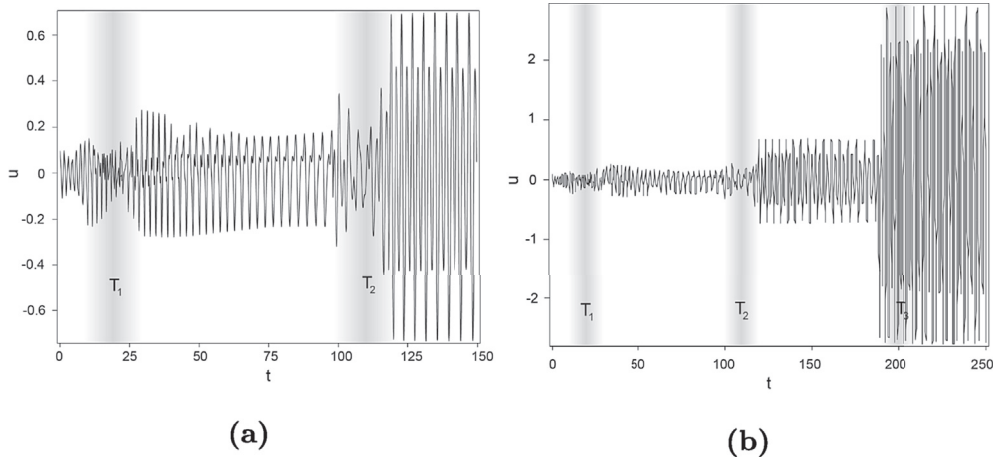


Fig. 3. Lateral displacements of the middle point of the cable up to the first three oscillation modes on timescales up to (a)  $t = 150$ , and (b)  $t = 250$ . The shadowed bands represent the resonance zones.

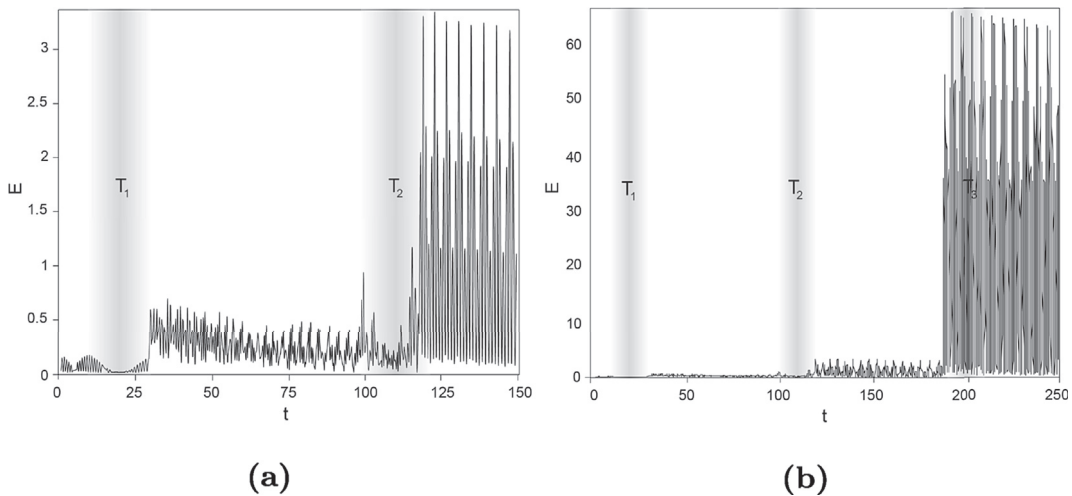


Fig. 4. Vibratory energy of the middle point of the cable up to the first three oscillation modes on timescales up to (a)  $t = 150$ , and (b)  $t = 250$ . The shadowed bands represent the resonance zones.

Figs. 3–4 depict the lateral displacements and the vibratory energy of the cable on timescales up to  $t = 150$  and  $t = 250$ . Note that subfigures (b) are simply enlarged version of subfigures (a), that is why all explanations for (b) are automatically inherent to (a). From the analytical results we can distinguish three main stages in time of resonance evolution such as the transition of the cable to the resonance zone, capture of the cable into resonance, and transition of the cable out of the resonance zone, the autoresonance stage, where the lateral displacements and the vibratory energy of the cable increases to a certain level and remains phase-locked until it meets another resonance zone. One can see this type of behavior in Figs. 3–4, where three resonances are detected corresponding to time instants  $T_1, T_2$ , and  $T_3$ . The shadowed bands represent the resonance layers which have the size of  $\mathcal{O}(\epsilon^{-\frac{1}{2}})$  as was obtained analytically. In the current example the resonance layers are found in the following intervals  $|t - T_i| \leq 10$  for  $i = 1, 2, 3$ . Note that in (a) and (b) these layers are visually different but with respect to the scale of the figures they are the same.

### 6.2. Numerical approximation

Since we neglected by bending stiffness, the governing equation (18a) for  $0 < \xi < 1$  takes the following form:

$$u_{tt} - \frac{1}{l^2} u_{\xi\xi} = -\epsilon \left( -\frac{2}{l} (1 - \xi) u_{\xi t} + \frac{\mu_0}{l} (1 - \xi) u_{\xi\xi} + \frac{\mu_0}{l} u_{\xi} + \xi I S_1 + S_2 \right), \tag{104}$$

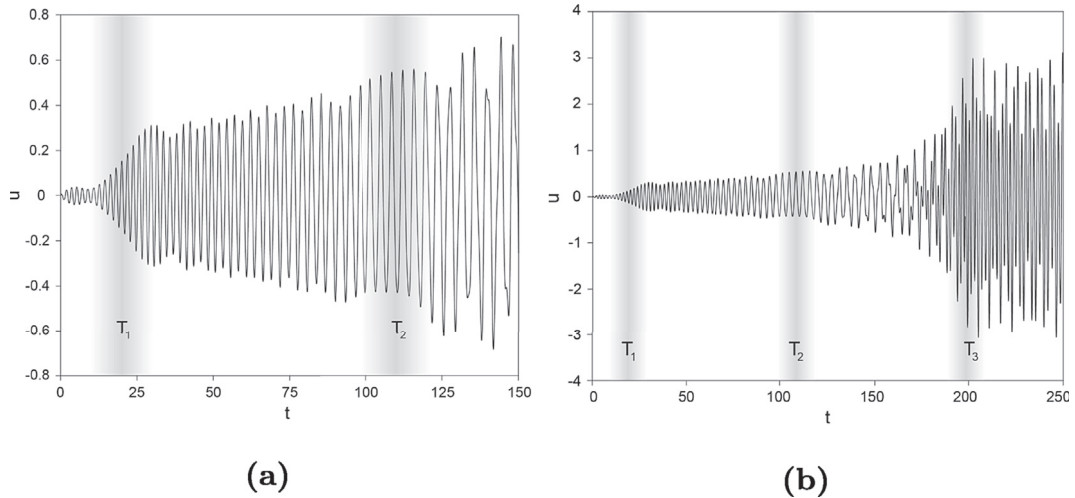


**Fig. 5.** Lateral displacements of the middle point of the cable up to the first three oscillation modes on timescales up to (a)  $t = 150$ , and (b)  $t = 250$ . The shadowed bands represent the resonance zones.

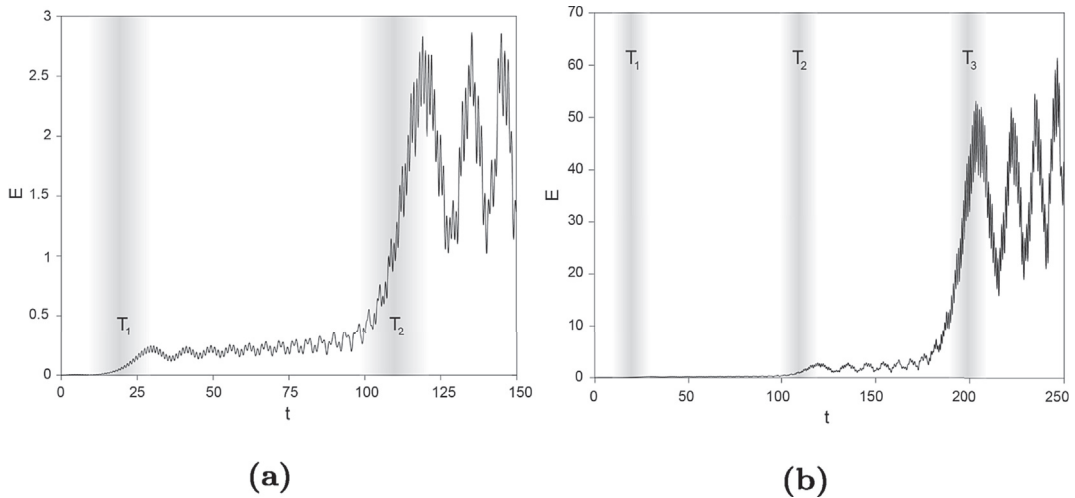


**Fig. 6.** Vibratory energy of the middle point of the cable up to the first three oscillation modes on timescales up to (a)  $t = 150$ , and (b)  $t = 250$ . The shadowed bands represent the resonance zones.

where the upper bar notation is omitted for convenience,  $S_1$  and  $S_2$  are given by (7) and (8). To solve (104) numerically, we first discretize it in space by using the central finite difference scheme. Then, we rewrite the so-obtained discretized equation in a matrix form and use the numerical time integration by the Crank-Nicolson method (see Appendix B). Note that the same values of parameters as for the analytic approximations are used here for computation. Thus, Figs. 5–6 show the lateral displacements and the vibratory energy of the cable, respectively, on timescales up to  $t = 150$  and  $t = 250$ . Note that as before Fig. 5 is enlarged Fig. 6. From these figures one can see that in the resonance zones the lateral displacements and the vibratory energy increase and, between these zones, stay phase-locked. We can make a conclusion that the general dynamic behavior of the solution approximated numerically is in agreement with the analytic approximation.

## 7. Conclusions and future results

In this paper, the lateral vibrations and resonances emerging in an elevator cable system due to the excitation at its boundaries initiated by the wind-induced building sway were studied. In order to prescribe the boundary conditions of the problem, the exact solution representing the sway of the building was found in Appendix A. Further, an initial-boundary value problem describing the lateral vibrations of a vertically moving beam with small bending stiffness and (in time) linear length variations was considered. In order to tackle the initial-boundary value problem and to construct a formal approximation of the solution, an advanced analytic scheme consisting of many elementary steps has been developed. From an internal layer analysis, it fol-

lowed that an additional natural timescale inside the resonance zone is  $\sqrt{\epsilon}t$ , and outside the resonance layer it is  $\epsilon t$ . Moreover, we also predicted exact instants of time when resonance emerged. Note that from the physical point of view resonance occurs, when the length of the cable becomes such that the one of the natural frequencies of its oscillations match with the fundamental frequency of the building sway (or boundary excitation). Further, we constructed an accurate approximation of the solution on a timescale of order  $\epsilon^{-1}$  by the three-timescales perturbation method, and the following conclusions could be drawn:

- order  $\epsilon$  boundary excitations of the cable result in  $\sqrt{\epsilon}$ -order vibration responses;
- the Fresnel integrals involved in the solution cause autoresonance phenomena in the system;
- since the solution contains infinitely many modes, there are infinitely many autoresonances in the system;
- for smaller  $\epsilon$  values, more time is needed to catch resonance and more time is needed to pass through a resonance zone;
- higher-order modes have smaller amplitudes (than lower order modes), carrying low impact into the system, due to the factor  $k^{-5/2}$  in the expressions for the amplitudes of vibrations in the  $\sqrt{\epsilon}$ -order approximation.

The numerical results confirmed these conclusions. Moreover, the constructed analytic approximations are in agreement with the numerical approximations.

The analytical scheme developed for this problem can readily be extended to other, more complicated and realistic, types of elevator motion. For instance, one can investigate the sway dynamics of the elevator cable under three different states of the elevator motion. The first state is acceleration, when the lift begins to accelerate from the resting position. Then, after acceleration, it can move at a constant velocity. Finally, the elevator decelerates before stopping at a certain floor. This example might add extra resonance manifolds and might produce new asymptotic timescales in the dynamics of the cable. One should be also aware of intersection of resonance zones [17], what makes the analysis of the problem even more interesting, but complex. In conclusion, the analytic methodology developed in this paper can be implemented in other types of gyroscopic systems which are governed by differential equations with in time slowly varying coefficients.

### Appendix A. Boundary sway

As it is mentioned in the introduction of this paper, the motion of the elevator cable's boundaries in horizontal direction is induced by the building sway. So, to prescribe the boundary conditions for the cable, we need to determine the exact solution of the building motion. We model the building as a vertical, cantilevered at the bottom, Euler-Bernoulli beam of length  $H$  (see Fig. 1). The PDE representing the motion of the building is given by a beam-like equation for  $0 < x < H$ , and  $t > 0$  as follows:

$$u_{tt} + u_{xxxx} = 0, \tag{105a}$$

subject to the boundary conditions:

$$u(0, t) = u_x(0, t) = 0, \tag{105b}$$

$$u_{xx}(H, t) = u_{xxx}(H, t) = 0,$$

for  $t > 0$ , and with the initial conditions:

$$u(x, 0) = \phi_1(x), \tag{105c}$$

$$u_t(x, 0) = \phi_2(x),$$

for  $0 < x < l_0$ .

This well-known IBV-problem can be solved by the method of separation of variables, where  $u(x, t) = X(x)T(t)$ , yielding

$$\frac{X^{(4)}}{X} = -\frac{\ddot{T}}{T} = \nu^2. \tag{106}$$

From (106) two equations, for  $T$  and  $X$ , follow. First, the equation for  $T$  is given by  $\ddot{T} + \nu^2 T = 0$ , for which the solution can be readily found as  $T(t) = A \cos \nu t + B \sin \nu t$ , where  $A$  and  $B$  are constants. For convenience we will use the following notation  $\lambda^4 = \nu^2$ . The mode-equation for  $X$  is given by  $X^{(4)} - \lambda^4 X = 0$ , which has a well-known solution  $X(x) = C_1 \sin \lambda x + C_2 \cos \lambda x + C_3 \sinh \lambda x + C_4 \cosh \lambda x$ , corresponding to the following roots of the characteristic equation  $\pm \lambda$  and  $\pm i\lambda$ . So using the boundary conditions (105b) and the fact of the existence of a non-trivial solution, we obtain the following equation for the eigenvalues  $1 + \cos \lambda_n H \cosh \lambda_n H = 0$ , which are actually the natural frequencies of the cantilever beam. This transcendental equation can be solved numerically, providing the following results  $\lambda_1 H = 1.875$ ,  $\lambda_2 H = 4.694$ ,  $\lambda_3 H = 7.855$ ,  $\lambda_4 H = 10.996$ ,  $\lambda_5 H = 14.137$ , ... . Corresponding eigenfunctions are given by  $X_n(x) = C_{1,n} \sin \lambda_n x + C_{2,n} \cos \lambda_n x + C_{3,n} \sinh \lambda_n x + C_{4,n} \cosh \lambda_n x$ . To find the constants of integration, we use the boundary conditions (105b). Then, the eigenfunctions are given by

$$X_n(x) = \sin(\lambda_n x) - \sinh(\lambda_n x) - \alpha_n (\cos(\lambda_n x) - \cosh(\lambda_n x)), \tag{107}$$

for  $n \in \mathbb{N}$ , where  $\alpha_n := \frac{\sin(\lambda_n H) + \sinh(\lambda_n H)}{\cos(\lambda_n H) + \cosh(\lambda_n H)}$ . A solution for  $T$  can be also rewritten in accordance with the eigenvalues as follows

$$T_n(t) = A_n \cos(\lambda_n^2 t) + B_n \sin(\lambda_n^2 t), \tag{108}$$

where  $A_n$  and  $B_n$  are constants following from the initial conditions (105c). Thus, the sway of the building is given by  $u(x, t) = \sum_{n=1}^{\infty} T_n(t)X_n(x)$  or in a full form, using (107)–(108), as follows:

$$u(x, t) = \sum_{n=1}^{\infty} (A_n \cos(\lambda_n^2 t) + B_n \sin(\lambda_n^2 t)) (\sin(\lambda_n x) - \sinh(\lambda_n x) - \alpha_n [\cos(\lambda_n x) - \cosh(\lambda_n x)]). \tag{109}$$

**Appendix B. Discretization and time integration**

Here we solve (104) numerically. In order to make the numerical integration easier, it is more convenient to rewrite this equation as a system of coupled first-order partial differential equations:

$$\begin{cases} u_t = v, \\ v_t = \frac{1}{l^2} v_{\xi\xi} - \epsilon \left( -\frac{2}{l}(1 - \xi)v_{\xi} + \frac{\mu_0}{l}(1 - \xi)u_{\xi\xi} + \frac{\mu_0}{l}u_{\xi} + \xi l S_1 + S_2 \right). \end{cases} \tag{110}$$

Next, let us use equispaced mesh grids  $\xi_j = j\Delta\xi$  for  $j = 1, 2, \dots, n$  with  $n\Delta\xi = 1$ . Introducing the differences,

$$\begin{aligned} u_{\xi}(\xi_j, t) &= \frac{u_{j+1} - u_{j-1}}{2\Delta\xi} + \mathcal{O}((\Delta\xi)^2), \\ u_{\xi\xi}(\xi_j, t) &= \frac{u_{j+1} - 2u_j + u_{j-1}}{(\Delta\xi)^2} + \mathcal{O}((\Delta\xi)^2), \\ v_{\xi}(\xi_j, t) &= \frac{v_{j+1} - v_{j-1}}{2\Delta\xi} + \mathcal{O}((\Delta\xi)^2), \end{aligned}$$

we discretize (110) as follows:

$$\begin{cases} \frac{du}{dt}(\xi_j, t) = v_j, \\ \frac{dv}{dt}(\xi_j, t) = r_j \frac{v_{j+1} - v_{j-1}}{2\Delta\xi} + q_j \frac{u_{j+1} - 2u_j + u_{j-1}}{(\Delta\xi)^2} - h \frac{u_{j+1} - u_{j-1}}{2\Delta\xi} - s_j, \end{cases} \tag{111}$$

where  $r_j := \frac{2\epsilon}{l}(1 - \xi_j)$ ,  $q_j := \frac{1}{l} \left( \frac{1}{l} - \epsilon\mu_0(1 - \xi_j) \right)$ ,  $h := \frac{\epsilon\mu_0}{l}$ , and  $s_j := \epsilon\xi_j l S_1 + S_2$  for  $j = 1, 2, \dots, n$ . Further, we denote a zero matrix by  $\emptyset$ , the identity matrix by  $I$ , and also introduce the following two matrices,

$$\begin{aligned} Q &:= \frac{1}{(\Delta\xi)^2} \begin{bmatrix} -2q_1 & q_1 - \frac{\Delta\xi}{2}h & 0 & \dots & \dots & 0 \\ q_2 + \frac{\Delta\xi}{2}h & -2q_2 & q_2 - \frac{\Delta\xi}{2}h & \ddots & & \vdots \\ 0 & \ddots & \ddots & \ddots & \ddots & \vdots \\ \vdots & \ddots & \ddots & \ddots & \ddots & 0 \\ \vdots & & \ddots & q_{n-1} + \frac{\Delta\xi}{2}h & -2q_{n-1} & q_{n-1} - \frac{\Delta\xi}{2}h \\ 0 & \dots & \dots & 0 & q_n + \frac{\Delta\xi}{2}h & -2q_n \end{bmatrix}, \\ R &:= \frac{1}{2\Delta\xi} \begin{bmatrix} 0 & r_1 & 0 & \dots & \dots & 0 \\ -r_2 & 0 & r_2 & \ddots & & \vdots \\ 0 & \ddots & \ddots & \ddots & \ddots & \vdots \\ \vdots & \ddots & \ddots & \ddots & \ddots & 0 \\ \vdots & & \ddots & -r_{n-1} & 0 & r_{n-1} \\ 0 & \dots & \dots & 0 & -r_n & 0 \end{bmatrix}, \end{aligned}$$

in  $\mathbb{R}^{n \times n}$ . The introduced four matrices compose a system matrix of (111) as follows:

$$M := \begin{bmatrix} \emptyset & I \\ Q & R \end{bmatrix} \in \mathbb{R}^{2n \times 2n}.$$

In addition, let us introduce the following vectors:

$$\begin{aligned} \mathbf{w} &= (u_1(\xi_1, t), u_2(\xi_2, t), \dots, u_n(\xi_n, t), v_1(\xi_1, t), v_2(\xi_2, t), \dots, v_n(\xi_n, t))^T, \\ \mathbf{s} &= (\underbrace{0, 0, \dots, 0}_n, s_1, s_2, \dots, s_n)^T. \end{aligned}$$

Thus, system (111) can be written in a matrix form as follows:

$$\frac{d\mathbf{w}}{dt} = \mathbf{M}\mathbf{w} - \mathbf{s}. \tag{112}$$

In order to perform a time integration of (112), we apply the Crank-Nicolson method; note that this method is basically based on the trapezoidal rule. Introducing the equispaced mesh grid in time  $t_k = k\Delta t$  for  $k = 1, 2, \dots, n$ , and using the Crank-Nicolson method, we obtain

$$\mathbf{w}^{k+1} = \mathbf{D}\mathbf{w}^k - \frac{\Delta t}{2} \frac{\mathbf{s}^{k+1} + \mathbf{s}^k}{\mathbf{I} - \frac{\Delta t}{2}\mathbf{M}^{k+1}}, \tag{113}$$

where  $\mathbf{D} \in \mathbb{R}^{2n \times 2n}$  is the amplification factor

$$\mathbf{D} = \frac{\mathbf{I} + \frac{\Delta t}{2}\mathbf{M}^k}{\mathbf{I} - \frac{\Delta t}{2}\mathbf{M}^{k+1}}, \tag{114}$$

and where the identity matrix  $\mathbf{I} \in \mathbb{R}^{2n \times 2n}$ .

### Appendix C. Energy

#### Analytic expressions

The total mechanical energy of the cable is given by

$$E(t) = \frac{1}{2} \int_0^l [\rho(u_t + v u_x)^2 + P u_x^2 + E l u_{xx}^2] dx, \tag{115}$$

where  $l = l(t)$ , and  $P$  is given by (2). Using the dimensionless quantities (3), we rewrite the energy in a dimensionless form:

$$E(t) = \frac{1}{2} \int_0^1 \left( (u_t + v u_x)^2 + \left( 1 + (\mu - \dot{v})(l - x) - \frac{\dot{v}}{\mu} \right) u_x^2 + p u_{xx}^2 \right) dx. \tag{116}$$

In order to define the energy on the interval (0, 1), we change variables by using the following transformation  $x = l\xi$ :

$$E(t) = \frac{1}{2} \int_0^1 \frac{1}{l} \left( (l u_t + v [1 - \xi] u_\xi)^2 + \left( 1 + l[\mu - \dot{v}][1 - \xi] - \frac{\dot{v}}{\mu} \right) u_\xi^2 + p u_{\xi\xi}^2 \right) d\xi. \tag{117}$$

#### Numerical integration

In order to compute integral (117) numerically, let us use the forward differences for  $u_\xi$  and  $u_{\xi\xi}$ , respectively:

$$u_\xi(\xi_i, t) = \frac{u_{i+1} - u_i}{\Delta\xi} + \mathcal{O}(\Delta\xi), \quad \text{and} \quad u_{\xi\xi}(\xi_i, t) = \frac{u_{i+2} - 2u_{i+1} + u_i}{(\Delta\xi)^2} + \mathcal{O}(\Delta\xi), \tag{118}$$

for  $i = 1, 2, \dots, n$ , and the trapezoidal rule for  $u_t$ :

$$u_t(\xi, t) = \kappa_i v_i + \kappa_{i+1} v_{i+1}, \tag{119}$$

where  $\kappa_i := \frac{\xi - \xi_{i+1}}{\xi_i - \xi_{i+1}}$  and  $\kappa_{i+1} := \frac{\xi - \xi_i}{\xi_{i+1} - \xi_i}$ . The integrals of  $u_\xi$ ,  $u_\xi^2$ , and  $u_{\xi\xi}^2$  over  $\xi$  can be readily computed. That is why we skip further details for this part and turn to the integration of  $u_t$  and  $u_t^2$ . Their integrals over  $\xi$  are computed by using (119) and the Holland-Bell theorem [18]:

$$\int_0^1 u_t d\xi = \sum_{i=1}^n \int_{\xi_i}^{\xi_{i+1}} (\kappa_i v_i + \kappa_{i+1} v_{i+1}) d\xi = \sum_{i=1}^n \frac{v_{i+1} + v_i}{2} \Delta\xi, \tag{120}$$

$$\int_0^1 u_t^2 d\xi = \sum_{i=1}^n \int_{\xi_i}^{\xi_{i+1}} (\kappa_i^2 v_i^2 + 2\kappa_i \kappa_{i+1} v_i v_{i+1} + \kappa_{i+1}^2 v_{i+1}^2) d\xi = \sum_{i=1}^n \frac{1}{3} \left( v_i^2 + \frac{1}{4} v_i v_{i+1} + v_{i+1}^2 \right) \Delta\xi. \tag{121}$$

## References

- [1] S.H. Sandilo, W.T. van Horssen, On a cascade of autoresonances in an elevator cable system, *Nonlinear Dyn.* 80 (3) (2015) 1613–1630, <https://doi.org/10.1007/s11071-015-1966-8>.
- [2] S. Kaczmarczyk, The passage through resonance in a catenary-vertical cable hoisting system with slowly varying length, *J. Sound Vib.* 208 (2) (1997) 243–265.
- [3] W.D. Zhu, J. Ni, Energetics and stability of translating media with an arbitrarily varying length, *J. Vib. Acoust. Trans. ASME* 122 (3) (2000) 295–304.
- [4] W. Zhu, G. Xu, Vibration of elevator cables with small bending stiffness, *J. Sound Vib.* 263 (2003) 679–699.
- [5] W.D. Zhu, L.J. Teppo, Design and analysis of a scaled model of a high-rise, high-speed elevator, *J. Sound Vib.* 264 (3) (2003) 707–731, [https://doi.org/10.1016/S0022-460X\(02\)01218-X](https://doi.org/10.1016/S0022-460X(02)01218-X).
- [6] S. Kaczmarczyk, W. Ostachowicz, Transient vibration phenomena in deep mine hoisting cables. Part 1: mathematical model, *J. Sound Vib.* 262 (2) (2003) 219–244, [https://doi.org/10.1016/S0022-460X\(02\)01137-9](https://doi.org/10.1016/S0022-460X(02)01137-9).
- [7] S. Kaczmarczyk, W. Ostachowicz, Transient vibration phenomena in deep mine hoisting cables. Part 2: numerical simulation of the dynamic response, *J. Sound Vib.* 262 (2) (2003) 245–289, [https://doi.org/10.1016/S0022-460X\(02\)01148-3](https://doi.org/10.1016/S0022-460X(02)01148-3).
- [8] W.D. Zhu, Y. Chen, Theoretical and experimental investigation of elevator cable dynamics and control, *J. Vib. Acoust. Trans. ASME* 128 (1) (2006) 66–78, <https://doi.org/10.1115/1.2128640>.
- [9] Y.F.H. Kimura, H. Ito, T. Nakagawa, Forced vibration analysis of an elevator rope with both ends moving, *J. Vib. Acoust. Trans. ASME* 129 (4) (2007) 471–477.
- [10] S. Kaczmarczyk, Nonlinear sway and active stiffness control of long moving ropes in high-rise vertical transportation systems, *Vibration Problems ICOVP 2011: the 10th International Conference on Vibration Problems*, Springer Proc. Phys. 139 (2011) 183–188.
- [11] P.P.R. Crespo, S. Kaczmarczyk, H. Su, The coupled nonlinear dynamics of a lift system, *AIP Conf. Proc.* 1637 (2014) 245.
- [12] C.-M. Zhang, J.-H. Bao, P. Zhang, W. Sun, Transverse vibration of flexible hoisting rope with time-varying length, *J. Mech. Sci. Technol.* 28 (2) (2014) 457–466.
- [13] N. Gaiko, W. van Horssen, On transversal oscillations of a vertically translating string with small time-harmonic length variation, *J. Sound Vib.* 383 (2016) 339–348.
- [14] J. Kevorkian, J.D. Cole, *Multiple Scale and Singular Perturbation Methods*, Applied Mathematical Sciences, 1996.
- [15] A. Nayfeh, P. Pai, *Linear and Nonlinear Structural Mechanics*, Wiley-VCH, 2002.
- [16] F. Verhulst, *Nonlinear Differential Equations and Dynamical Systems*, Springer-Verlag, 1996.
- [17] F. Verhulst, Profits and pitfalls of timescales in asymptotics, *SIAM Rev.* 57 (2) (2015) 255–274.
- [18] I. Holand, K.B. Barber (Eds.), *Finite Element Methods in Stress Analysis*, 1969. Tapir.